Supplementary Materials for

Synergistic Engineering of Energetic Materials: From Molecular Design to Advanced Manufacturing

Haoran Liu, Chunlin Zhao, Qingyan Pan*,Ning Wang*

(Norinco Group Qingyang Chemical Industry Corporation, Liaoyang 111002)

Nitro-Containing Compounds

Table S1. The properties of some nitrate ester compounds.

Compounds	ρ, g/cm^3	Q, J/g	V_d, m/s	P_d, GPa	IS, J	Ref.
NC	1.64	4300	6970	20.8	3.0	[1]
NCh	1.68	7832	7810	24.0	14.2	[1]
NG(l)	1.60	6214	8030	26.5	0.2	[2]
PETN	1.77	6350	8710	33.0	5.1	[2]

Q: heat of explosion, V_d: detonation velocity, P_d: Explosion pressure, I_e: impact sensitivity.

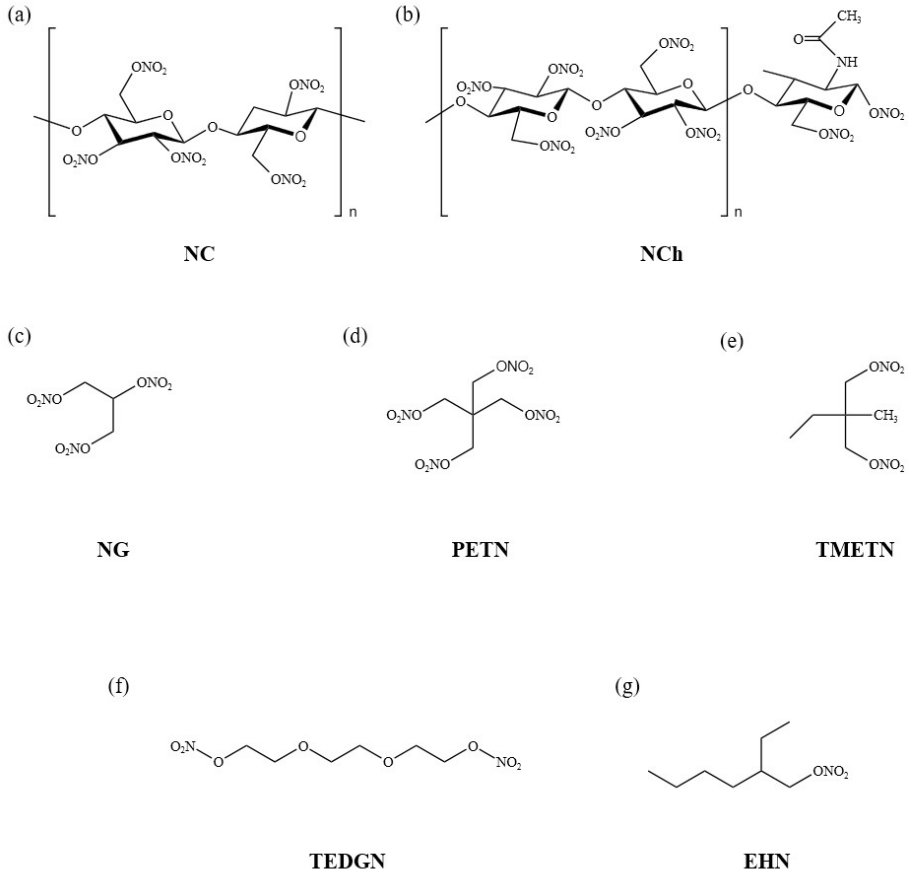

Figure S1. Molecular Structures of Nitrate Esters: (a) Nitrocellulose (NC), (b) Nitrochitosan (NCh), (c) Nitroglycerin (NG), (d) Pentaerythritol Tetranitrate (PETN), (e) Trimethylolethane Trinitrate (TMETN), (f) Triethylene Glycol Dinitrate (TEGDN), (g) 2-Ethylhexyl Nitrate (EHN).

Table S2. The properties of some nitramines compounds.

Compounds	ρ, g/cm^3	Q, J/g	V_d, m/s	P_d, GPa	IS, J	Ref.
RDX	1.81	5350	8748	34.9	5.6	[3]

HMX	1.91	5680	9320	39.5	6.4	[4]
CL-20	2.05	6300	9406	44.6	4.1	[5]

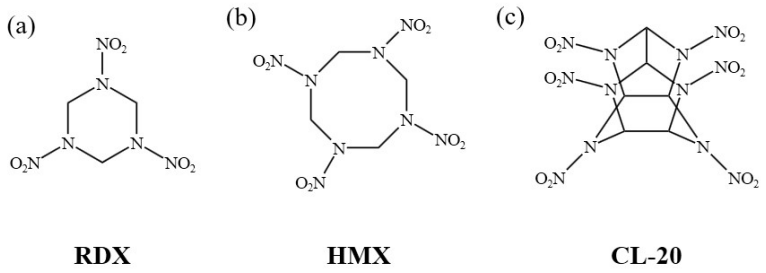

Figure S2. Molecular Structures of Nitramines: (a) Hexogen (RDX), (b) Octogen (HMX) (c) Hexanitrohexaazaisowurtzitane (CL-20).

Table S3. The properties of some nitrocarbon compounds.

Compounds	ρ, g/cm^3	Q, J/g	V_d, m/s	P_d, GPa	IS, J	Ref.
TNT	1.65	4184	6820	19.5	15	[6]
TNP	1.81	5400	7830	27.2	7.4	[6]
TNA	1.77	4300	7523	24.8	22	[7]
HNB	1.93	7774	9330	40.2	< 1	[8]
TATB	1.94	3200	8540	32.1	50	[9]
NM(l)	1.14	4200	6200	11.2	10	[10]
TNM	1.62	2076	6368	14.8	0.4	[11]
FOX-7	1.89	4860	8930	34.0	60	[12]

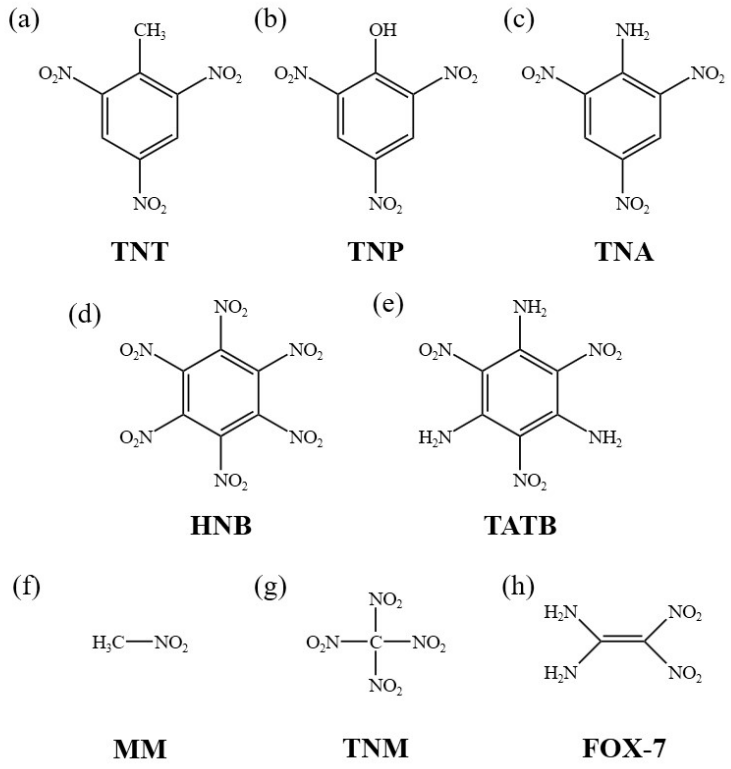

Figure S3. Molecular Structures of Nitrocarbon: (a) Trinitrotoluene (TNT), (b) Trinitrophenol (TNP) (c) Trinitroaniline (TNA), (d) Hexanitrobenzene (HNB), (e) 1,3,5-triamino-2,4,6-trinitrobenzene (TATB), (f) Nitromethane (MM), (g) Tetranitromethane (TNM), (h) 1,1-diamino-2,2-dinitroethylene (FOX-7)

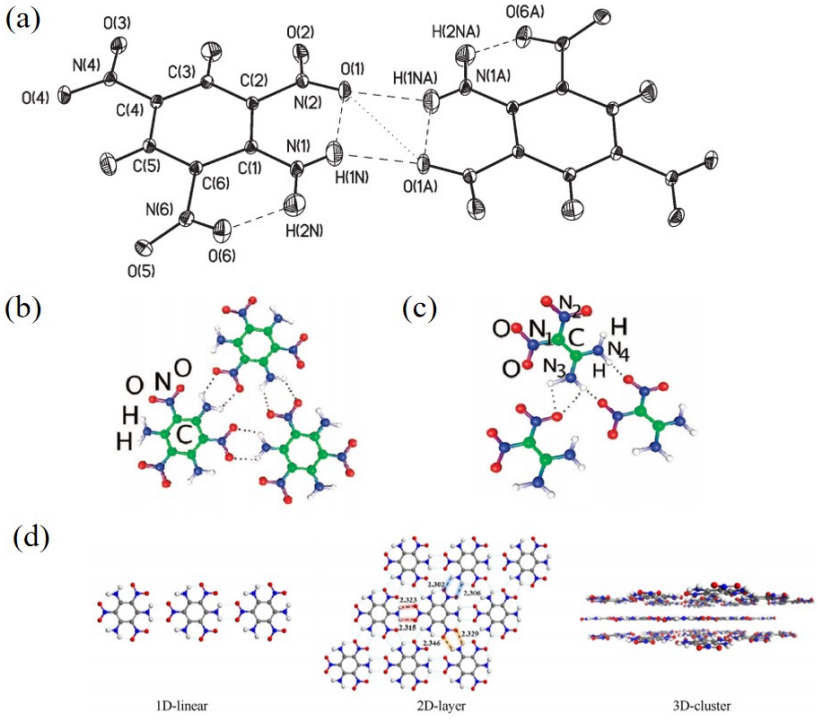

Figure S4. (a) Thermal ellipsoid representation of TNA dimers within the crystal lattice [13].

Copyright 2013, RSC (b) Layered molecular packing of TATB in the crystalline state [14]. (c) Layered arrangement of FOX-7 molecules within the crystal structure [14]. Copyright 2008, ACS (d) Schematic illustration of TATB cluster extraction across varying dimensional scales [15]. Copyright 2023, Elsevier.

Nitrogen-Rich Compounds

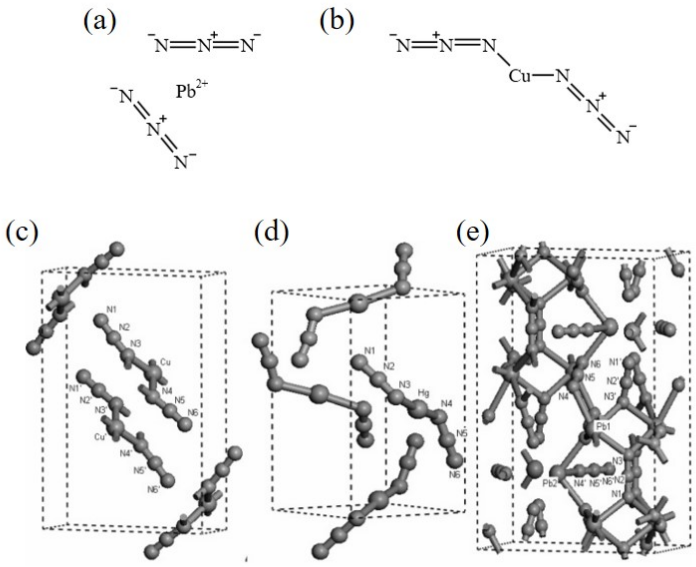

Figure S5. Electronic formula for (a) $Pb(N_3)_2$ (ionic compound), (b) $Cu(N_3)_2$ (covalent compound). Unit cells for (c) $Cu(N_3)_2$, (d) $Hg(N_3)_2$, and (e) $Pb(N_3)_2$. Big spheres stand for metal cations, and small spheres, nitrogen anions [16]. Copyright 2006, ACS.

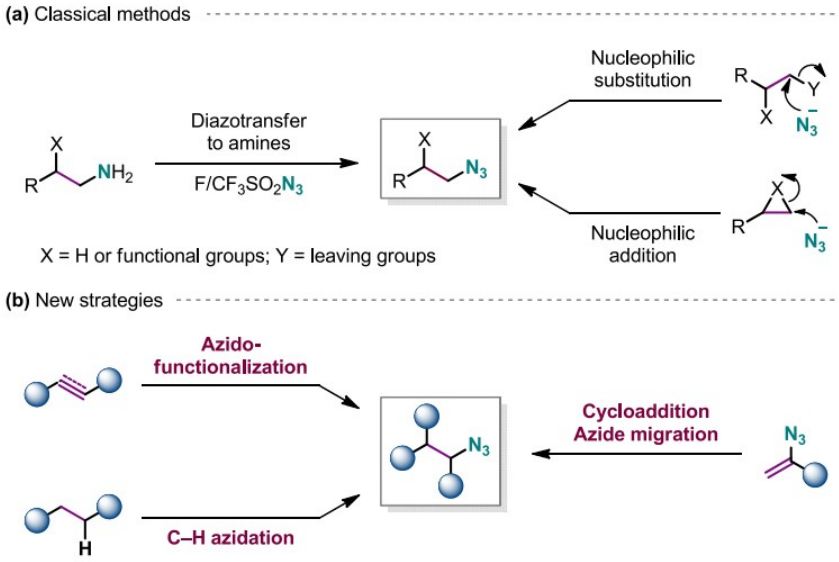

Figure S6. Strategies for the preparation of aliphatic azides [17]. Copyright 2021, ACS.

Table S4. The properties of N+ 5 ionic compounds.

Compounds	ρ, g/cm^3	△H f,, J/g	V_d, m/s	P_d, GPa	Td, ℃	Ref.
[N+ 5][NO-3]	1.81	4400	8642	30.3		[18]

[N+ 5][N(NO2)-2]	1.88	4200	8859	32.3		[18]
N+ 5N- 3	1.55	9020	9290	34.67		[19]
N+ 5N- 5	1.80	8450	10210	45.56		[19]

$\triangle H_f$ Heat of formation.

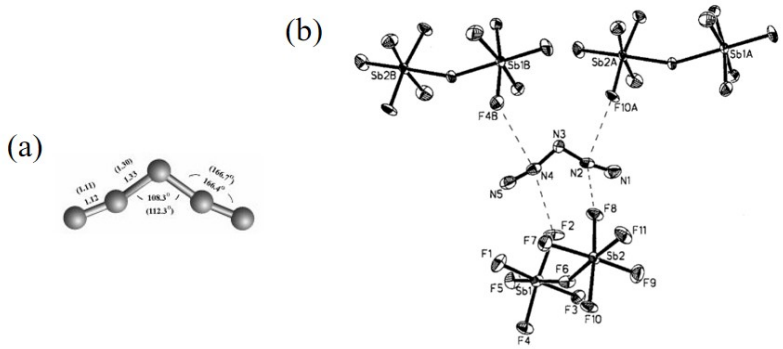

Figure S7. (a) Optimized structures of N+ 5 calculated at the B3LYP (values given in parentheses)and CCSD(T)/6-311+G(2d) levels of theory [20]. Copyright 1999, John Wiley and Sons Ltd. (b) ORTEP diagram of N+ $5Sb_2F$- 11, showing the thermal ellipsoids at the 30% probability level and the close-range N…F contacts within the crystal lattice [21]. Copyright 2001, ACS.

Table S5. The properties of N- 5 ionic compounds.

Compounds	ρ, g/cm^3	$\triangle$H f,, J/g	V_d, m/s	P_d, GPa	Td, °C	Ref.
$[N(CH_3)4]N$- 5	1.25	2064	5880	10.1	81	[22]
$[(N_2H_3)_2CNH_2]^+N$- 5	1.44	4806	7505	21.2	101	[23]
$(NH_4)^+N$- 5	1.49	7118	7757	23.2	106	[23]
$[NH_3C(NH)_2CH_2COOH]^+N$- 5	1.52	502.2	7392	18.1	108	[24]
$[Fe(H_2O)_4(N_5)_2]\cdot 4H_2O$	1.58				115	[25]
$[Mn(H_2O)_4(N_5)_2]\cdot 4H_2O$	1.59				104	[25]
$(NH_3OH)^+N$- 5	1.60	6438	9005	32.7	106	[23]
$(N_2H_5)^+N$- 5	1.62	4576	10400	37.0	85	[22]
$[C_2N_3H_2C(NH_2)_2]^+N$- 5	1.62	3217	8187	22.9	96	[26]
$[Zn(H_2O)_4(N_5)_2]\cdot 4H_2O$	1.65				108	[27]
$[C_7N_8H_2(NH_2)_4NO_2]^+N$- 5	1.70	2868	8124	23.7	111	[28]
KN_5	196	4592	6977	20.9	110	[23]

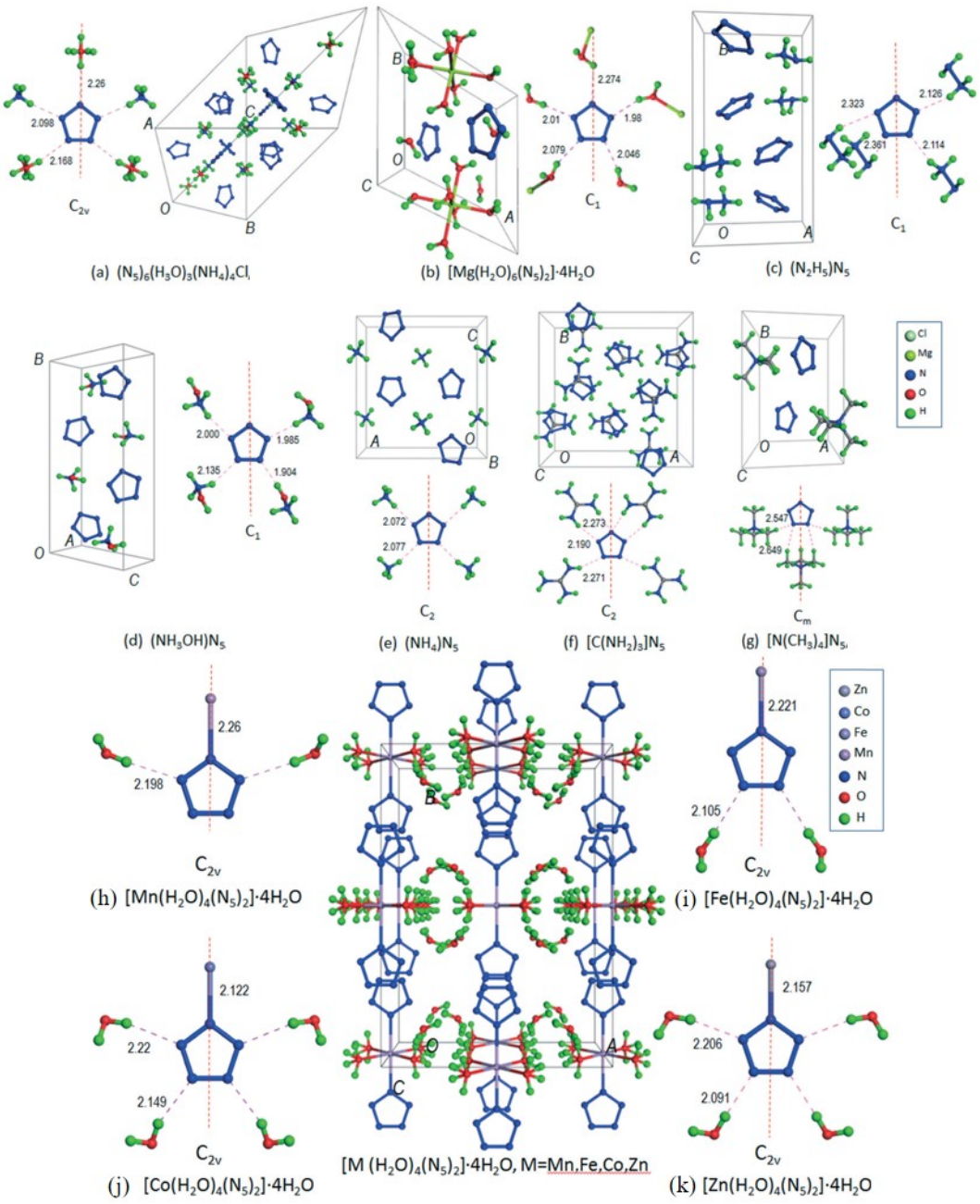

Figure S8. Bonding of cyclo-N- 5 and molecular stacking of group I,II [29]. Copyright 2019, RSC.

Nitrogen-containing heteroaromatics

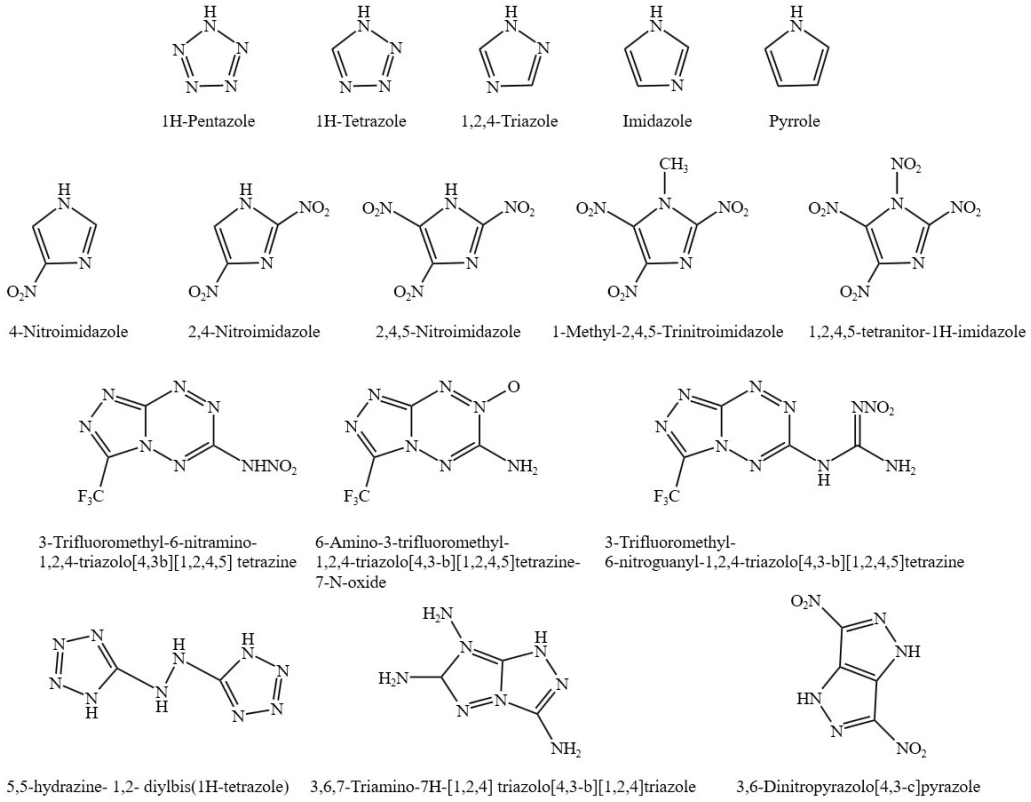

Figure S9. Molecular structures of some azole compounds and derivatives

Table S6. The properties of Azole compounds.

Compounds	ρ, g/cm^3	△H f,, J/g	V_d, m/s	P_d, GPa	IS, J	Ref.
1H-Tetrazole	1.53	2495	7813	21.0	<4	[30]
4-Nitroimidazole	1.56		6860	19.1	22.6	[31]
2,4-Nitroimidazole	1.75		8130	29.0	51.4	[31]
2,4,5-Trinitroimidazole	1.88		8980	36.7	14.2	[31]
1-Methyl-2,4,5-Trinitroimidazole	1.77		8130	28.1	14.6	[32]
1,2,4,5-tetranitor-1H-imidazole	1.90	1519	9437	39.0	＜1	[33]
3-Trifluoromethyl-6-nitramino-1,2,4-triazolo[4,3b][1,2,4,5]tetrazine	1.75		7179	20.8	10	[34]
6-Amino-3-trifluoromethyl-1,2,4-triazolo[4,3-b][1,2,4,5]tetrazine- 7-N-oxide	1.79		6925	18.8	36	[34]
3-Trifluoromethyl-6-nitroguanyl-1,2,4-triazolo[4,3-b][1,2,4,5] tetrazine	1.90		7877	26.8	＞60	[34]
5,5-hydrazine-1,2- diylbis(1H-tetrazole)	1.84	414	8523	27.7	＞30	[35]

3,6,7-Triamino-7H-[1,2,4] triazolo[4,3-b][1,2,4]triazole	1.73	3060	8580	25.9	40	[36]
3,6-Dinitropyrazolo[4,3-c]pyrazole	1.85	1940	8250	27.4	15	[37]

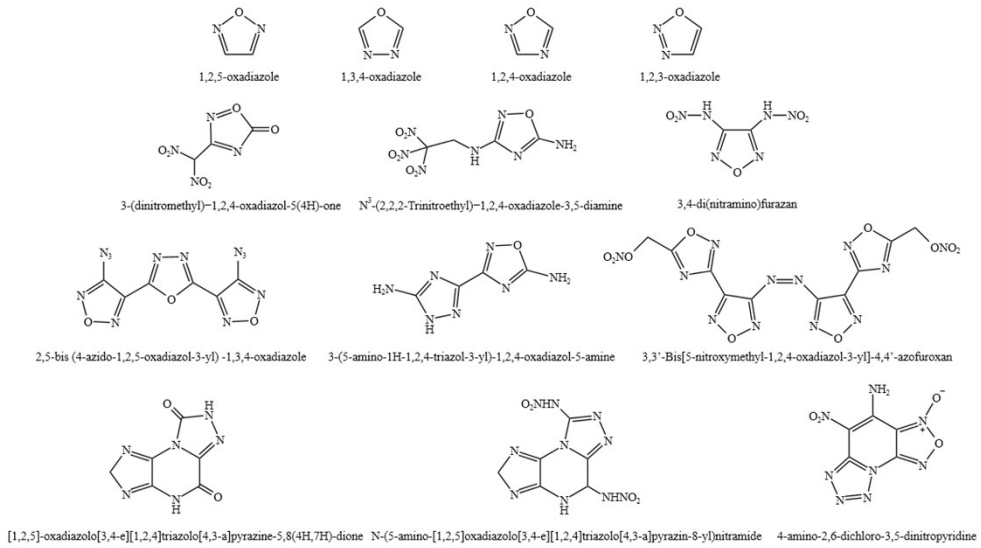

Figure S10. Molecular structures of some oxazoles compounds and derivatives.

Table S7. The properties of oxazoles compounds.

Compounds	ρ, g/cm^3	△H f,, J/g	V_d, m/s	P_d, GPa	IS, J	Ref.
3-(dinitromethyl)−1,2,4-oxadiazol-5(4H)-one	1.71	2130	7937	24.5	13	[38]
N^3-(2,2,2-Trinitroethyl)−1,2,4-oxadiazole-3,5-diamine	1.80		8500	31.2	6	[39]
3,4-di(nitramino)furazan	1.90	1510	9376	40.5	< 1	[40]
2,5-bis (4-azido-1,2,5-oxadiazol-3-yl) -1,3,4-oxadiazole	1.76	4720	8728	31.2	21.9	[41]
3-(5-amino-1H-1,2,4-triazol-3-yl)-1,2,4-oxadiazol-5-amine	1.78	1672	7871	21.8	＞40	[42]
3,3'-Bis[5-nitroxymethyl-1,2,4-oxadiazol-3-yl]-4,4'-azofuroxan	1.78	3389	8081	27.4	35	[43]
N-(5-amino-[1,2,5]oxadiazolo[3,4-e][1,2,4]triazolo[4,3-a]pyrazin-8-yl)nitramide	1.83	2540	8530	30.1	26	[44]
[1,2,5]-oxadiazolo[3,4-	1.84	570	7984	24.9	22	[44]

e][1,2,4]triazolo[4,3-a]pyrazine-5,8(4H,7H)-dione						
4-amino-2,6-dichloro-3,5-dinitropyridine	1.92	3815	8838	36.0	3	[45]

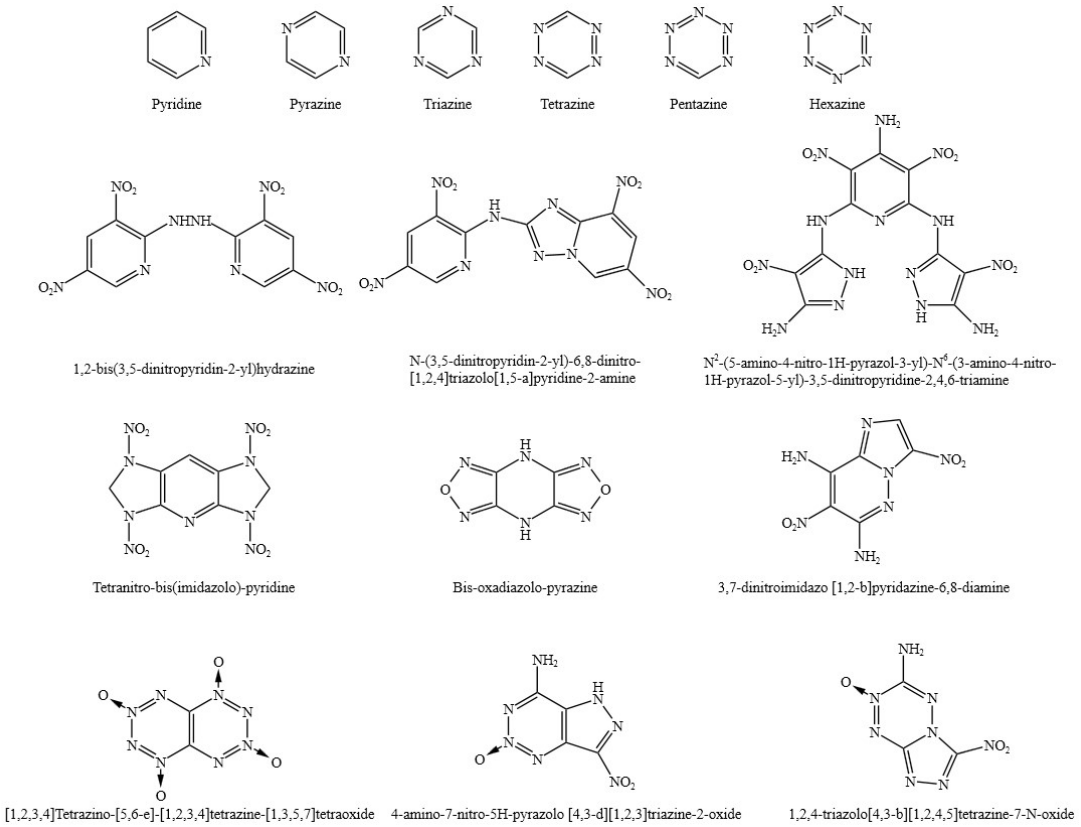

Figure S11. Molecular structures of some pyrimidine compounds and derivatives.

Table S8. The properties of pyrimidine compounds.

Compounds	ρ, g/cm^3	△H f,, J/g	V_d, m/s	P_d, GPa	IS, J	Ref.
1,2-bis(3,5-dinitropyridin-2-yl)hydrazine	1.74	973	7862	25.4	> 40	[46]
N-(3,5-dinitropyridin-2-yl)-6,8-dinitro-[1,2,4]triazolo[1,5-a]pyridine-2-amine	1.80	1196	8024	26.9	> 40	[46]
N^2-(5-amino-4-nitro-1H-pyrazol-3-yl)-N^6-(3-amino-4-nitro-1H-pyrazol-5-yl)-3,5-dinitropyridine-2,4,6-triamine	1.90	1911	8889	33.9	35	[47]

Tetranitro-bis(imidazolo)-pyridine	1.90	1351	8560	33.6	-	[48]
Bis-oxadiazolo-pyrazine	1.77	2333	7380	24.0	9.8	[49]
3,7-dinitroimidazo [1,2-b]pyridazine-6,8-diamine	1.80	1876	8434	27.7	> 40	[50]
[1,2,3,4]Tetrazino-[5,6-e]-[1,2,3,4]tetrazine-[1,3,5,7]tetraoxide	2.00	1000	10900	60.0	-	[51]
4-amino-7-nitro-5H-pyrazolo [4,3-d][1,2,3]triazine-2-oxide	1.84	2070	8731	31.2	>20	[52]
1,2,4-triazolo[4,3-b][1,2,4,5]tetrazine-7-N-oxide	1.86	3760	9320	39.5	7	[53]

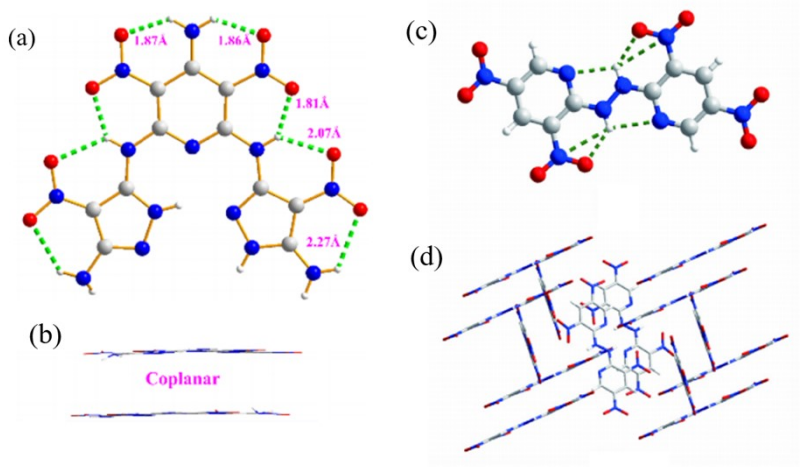

Figure S12. (a) (b)intramolecular hydrogen bond strengths and intermolecular conjugation structure of N^2-(5-amino-4-nitro-1H-pyrazol-3-yl)-N^6-(3-amino-4-nitro-1H-pyrazol-5-yl)-3,5-dinitropyridine-2,4,6-triamine[47]，(c) (d)Intramolecular hydrogen-bond and Stacking diagram of 1,2-bis(3,5-dinitropyridin-2-yl)hydrazine[46]. Copyright 2022, Elsevier.

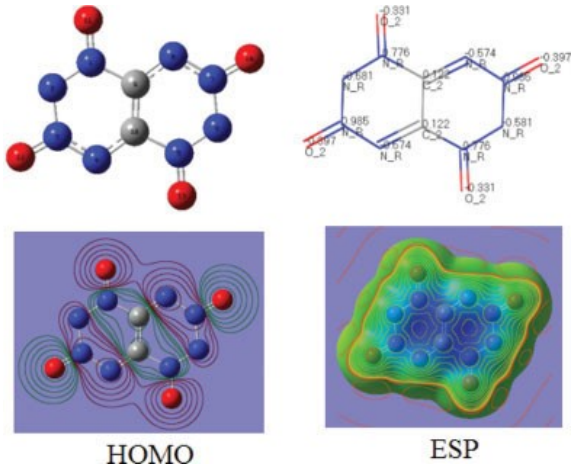

Figure S13. Molecular structure, Dreiding atomic types and CHelpG atomic charges, HOMO, and ESP of TTTO[51].

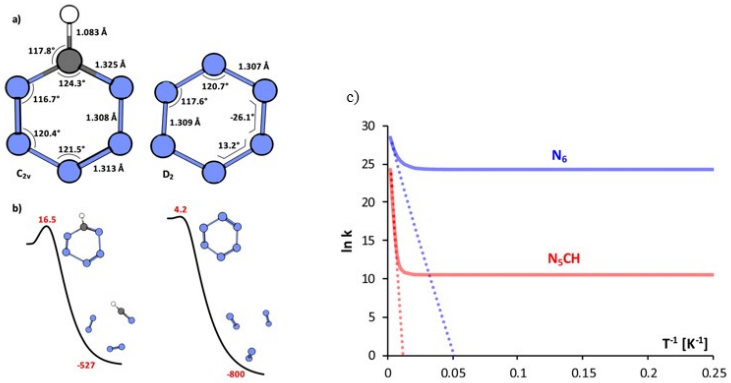

Figure S14. Pentazine (C_{2V}) and hexazine (D_2) stable geometries computed with MN15/Def2TZVP (a) and their decomposition paths (b). Relative energies + ZPE (kJ/mol) are presented in red.(c) Semi-classical (dashed lines) and tunneling included (solid lines) Arrhenius plots of hexazine and pentazine [54]. Copyright 2024, RSC.

Cage-Structured Frameworks

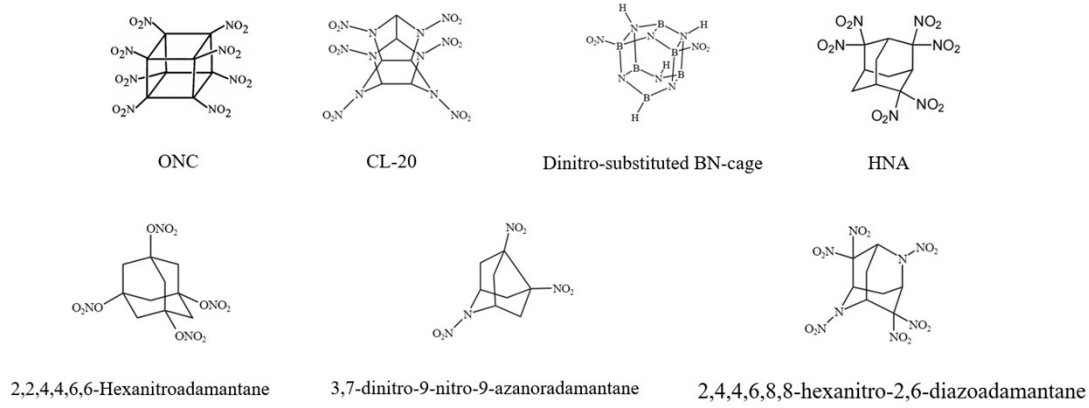

Figure S15. Some cage like molecular structures with high energy density

Table S9. The properties of cage like molecular structures compounds.

Compounds	ρ, g/cm^3	△H f,, J/g	V_d, m/s	P_d, GPa	IS, J	Ref.
ONC	2.19	862	10800	52.1		[55]
CL-20	2.05	2178	9406	44.6	4.1	[56]
dinitro-substituted BN-cage	1.93	547	7223	25.0	12.3	[57]
HNA	1.78	226	8443	33.0		[58]
2,2,4,4,6,6-Hexanitroadamantane	1.71	1529	7282	22.9	10	[59]
3,7-dinitro-9-nitro-9-azanoradamantane	1.65	160	7157	19.9		[60]

2,4,4,6,8,8-hexanitro-2,6-diazoadamantane	1.96	416	9310	40.3	[61]

Energetic Ionic Compounds

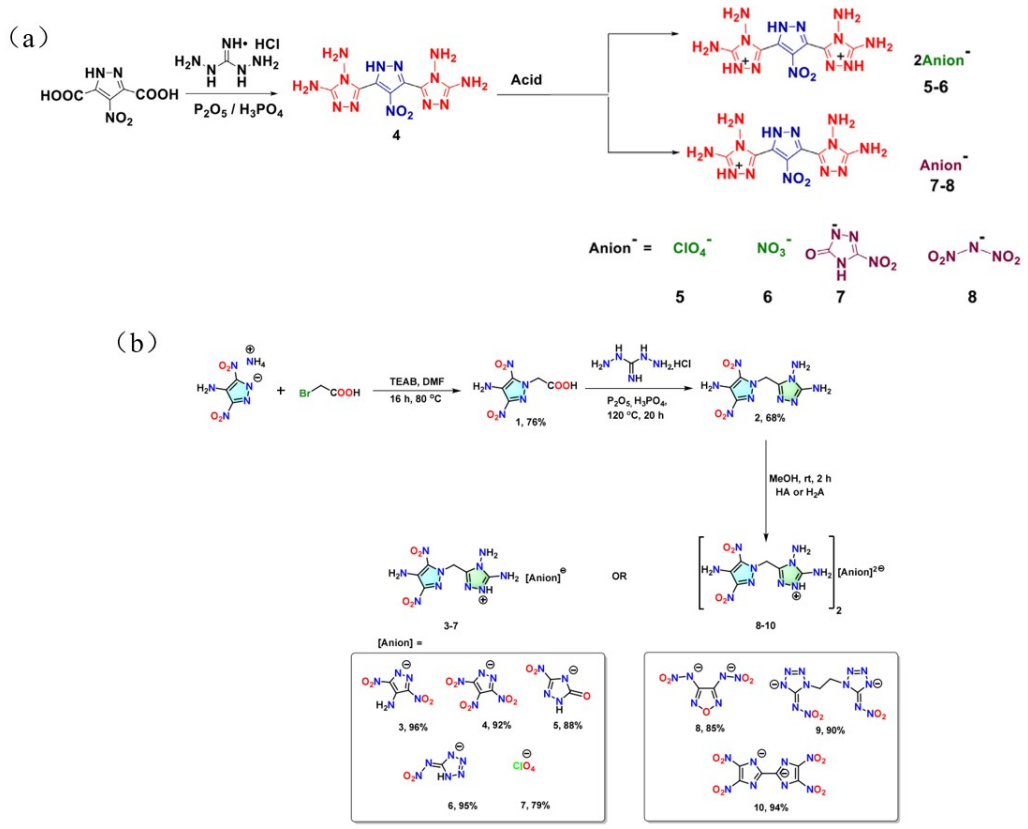

Figure S16. Molecular structure of organic ion energetic materials[62, 63]. Copyright 2021, 2024 Elsevier and ACS.

Table S10. The properties of organic ion energetic compounds [62, 63].

Compounds	T_d, °C	ρ, g/cm^3	ΔH f,, kJ/mol	V_d, m/s	P_d, GPa	IS, J	FS, N	Ref.
a-4	318.6	1.73	923	8197	24.2	> 40	> 360	[62]
a-5	304.2	1.83	243	8133	28.2	> 40	> 360	[62]
a-6	235.2	1.79	135	8266	26.3	> 40	> 360	[62]
a-7	255.6	1.76	800	8008	23.9	> 40	> 360	[62]
a-8	195.3	1.79	1040	8716	30.3	32	280	[62]
b-2	210	1.74	347	7783	23.0	> 40	> 360	[63]
b-3	270	1.78	576	8166	26.4	> 40	> 360	[63]
b-4	219	1.83	559	8441	30.1	> 40	> 360	[63]
b-5	212	1.74	674	8122	26.1	> 40	> 360	[63]
b-6	211	1.79	769	8480	28.2	> 40	> 360	[63]

b-7	212	1.85	318	8415	30.5	> 40	> 360	[63]
b-8	219	1.75	1925	8519	29.7	5	80	[63]
b-9	220	1.77	1097	8084	24.7	> 40	> 360	[63]
b-10	250	1.81	1165	8203	27.1	> 40	> 360	[63]

FS Friction sensitivity

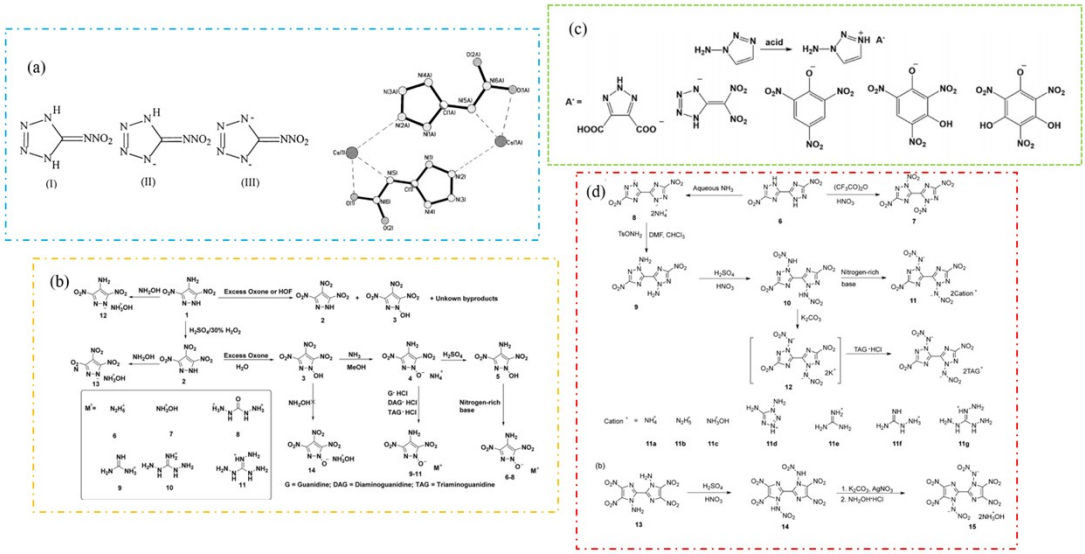

Figure S17. Molecular structure of organic ion energetic materials [64-67]. Copyright 2002, 2015, 2017, and 2018 Elsevier and Wiley-VCH Verlag GmbH & Co. KGaA.

Table S11. The properties of organic ion energetic compounds.

Compounds	T_d, ℃	ρ, g/cm^3	△H f,, J/g	V_d, m/s	P_d, GPa	IS, J	FS, N	Ref.
b-5H_2O	93	1.86				20	240	[65]
b-6	216	1.79	840	8935	34.4	25	240	[65]
b-7	182	1.86	360	9004	37.6	35	360	[65]
b-8	175	1.84	360	8797	34.0	40	360	[65]
b-9	204	1.71	50	8200	26.4	40	360	[65]
b-10	169	1.71	790	8540	28.0	40	360	[65]
b-11	214	1.75	1150	8877	30.7	40	360	[65]
b-12	212	1.80	540	8810	33.9	40	360	[65]
b-13	129	1.86	440	9135	38.0	25	240	[65]
c-1	151	1.69	-76	6699	19.2	40		[66]
c-2	149	1.77	263	7818	26.8	6.5		[66]
c-3	148	1.72	408	7742	25.9	40		[66]
c-4	162	1.71	204	7687	25.4	40		[66]

c-5	131	1.87	69	8231	30.7	28		[66]
d-9	271	1.83	440	8677	31.8	40	360	[67]
d-10	121	1.88	592	9243	38.2	3	40	[67]
d-11a	223	1.77	435	8769	33.1	10	120	[67]
d-11b	170	1.81	747	9170	36.4	7	120	[67]
d-11c	166	1.86	536	9330	39.1	8	120	[67]
d-11d	160	1.79	1668	9131	35.5	5	80	[67]
d-11e	252	1.74	432	8456	28.4	40	360	[67]
d-11f	197	1.72	680	8570	28.9	40	360	[67]
d-11g	200	1.73	1124	8927	31.3	10	160	[67]
d-14	116	1.94	481	9350	40.1	3	40	[67]
d-15	135	1.85	449	9169	38.2	6	80	[67]

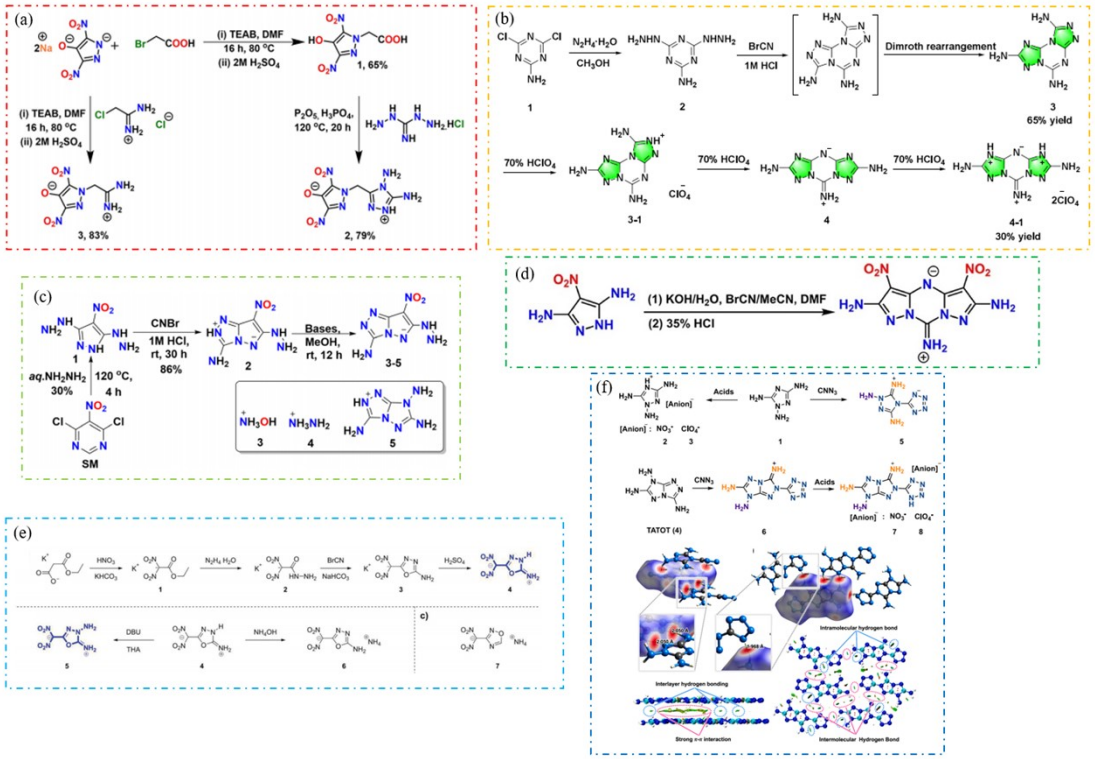

Figure S18. Molecular structure of zwitterionic energetic materials [68-73]. Copyright 2020, 2023, and 2024 ACS, RSC and Elsevier.

Table S12. The properties of organic ion energetic compounds.

Compounds	T_d, ℃	ρ, g/cm^3	△H f,, kJ/mol	V_d, m/s	P_d, GPa	IS, J	FS, N	Ref.
a-2	212	1.79	325.6	8085	25.8	> 40	> 360	[68]
a-3	270	1.73	60.7	7731	23.7	> 40	> 360	[68]
b-3	277	1.69	406.3	7226	17.1	> 40	> 360	[68]

b-3-1	325	1.81	517.5	8048	26.21	> 40	> 360	[68]
b-4	294	1.73	380.3	7360	17.77	> 40	> 360	[68]
b-4-1	309	1.89	428.1	8520	32.53	> 40	> 360	[68]
c-2	250	1.83	361.7	8409	26.14	10	> 360	[69]
c-3	262	1.78	460.4	8956	30.29	10	> 360	[69]
c-4	171	1.77	554.5	9163	31.16	10	> 360	[69]
c-5	240	1.77	948.8	8591	26.93	10	> 360	[69]
d-1	380	1.85	314.1	8390	27.2	> 40	> 360	[70]
e-4	211	1.75	378.5	8027	27.5	22	240	[71]
e-5	202	1.76	417.0	8375	30.6	16	200	[71]
e-6	121	1.76	380.7	8016	28.1	9.8	120	[71]
e-7	250	1.64	1090.7	8897	35.2	10	120	[71]
e-8	170	184	480.3	9014	36.7	1.5	80	[71]
e-9	174	1.74	448.5	8392	31.2	22	260	[71]
f-3	235	2.05	-203.2	9035	33.0	10	80	[72]
f-4	138	1.87	62.0	8828	34.6	25	120	[72]
f-5	143	1.87	139.1	8928	35.9	28	128	[72]
f-6	202	1.78	-72.2	8554	30.1	20	160	[72]
f-7	140	1.74	-29.7	8554	39.4	9	144	[72]

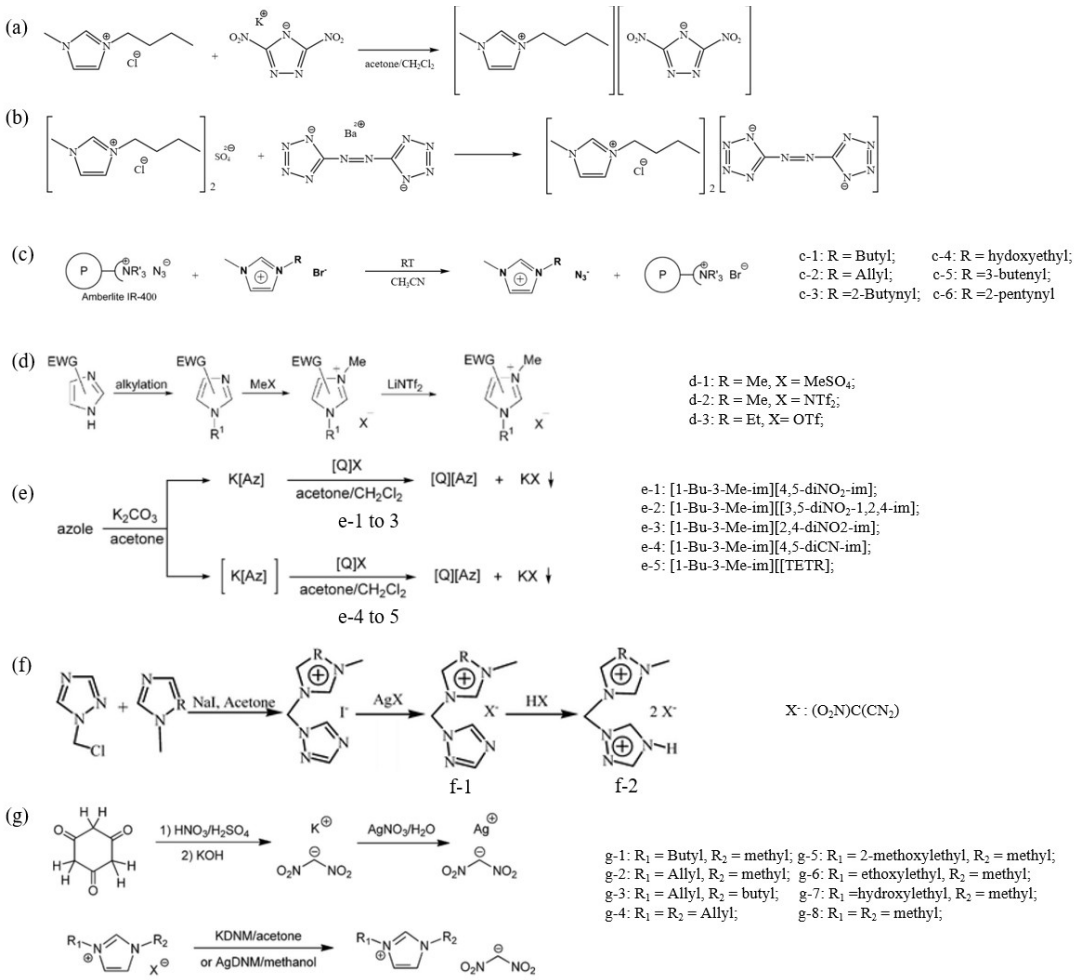

Figure S19. Molecular structure of imidazole based energetic ionic liquids.

Table S13. The properties of The properties of some imidazole based energetic ionic liquids.

EILs	T_m, ℃	T_g, ℃	T_d, ℃	ρ, g/cm^3	△H f,, kJ/mol	V_d, m/s	P_d, GPa	Ref.
a	35-36		239					[74]
b	3			1.26	-1006			[75]
c-1	36	-74	222		304			[76]
c-2	36	-3	214		167			[76]
c-3	19	-77	150		448			[76]
c-4	45	-57	188		423			[76]
c-5	66		115		598			[76]
c-6	19	-55	107		582			[76]
d-1	95		166	1.63	-			[77]
d-2	72		248	-	-			[77]
d-3	92		260	1.68	-			[77]
e-1		-64	241	-	-			[78]
e-2	33		239	-	-			[78]

e-3		-53	254	-	-			[78]
e-4		-74	230	-	-			[78]
e-5		-82	208	-	-			[78]
f-1	89		274	1.41	-			[79]
f-2	95		220	1.43	385.4	6063	11.1	[79]
g-1		-83	164	1.21				[80]
g-2		-73	162	1.36				[80]
g-3		-73	164	1.18				[80]
g-4		-79	166	1.23				[80]
g-5		-73	162	1.34				[80]
g-6		-62	154	1.38				[80]
g-7		-67	158	1.38				[80]
g-8	60		177	1.45				[80]

T_m Melting point, T_g Glass transition temperature.

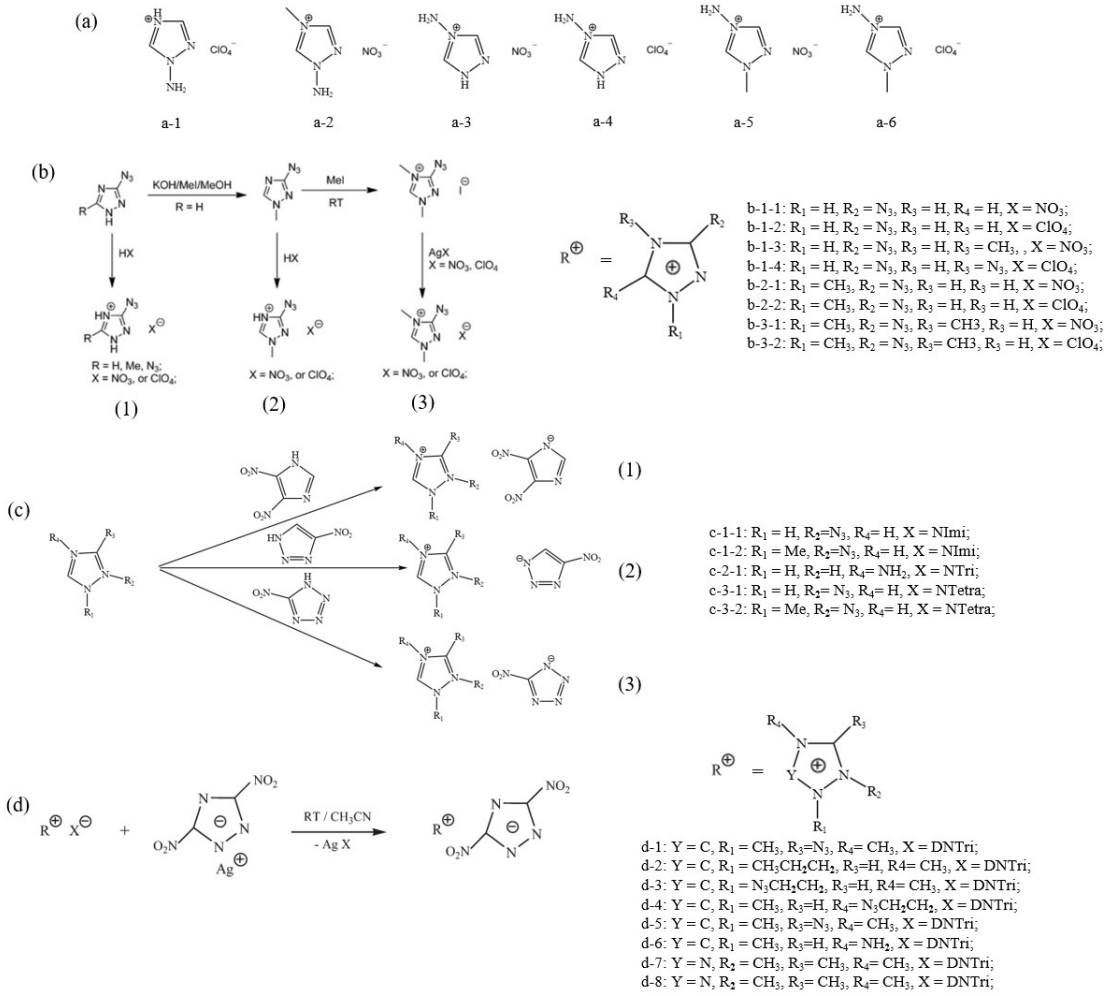

Figure S20. Molecular structure of triazole imidazole based energetic ionic liquids.

Table S14. The properties of some triazole imidazole based energetic ionic liquids.

EILs	T_m, ℃	T_g, ℃	T_d, ℃	ρ, g/cm^3	△H f,, kJ/mol	V_d, m/s	P_d, GPa	Ref.
a-1	91		235	1.80	357.01			[81]
a-2		-62	217	1.51	-174.68			[81]
a-3	69		181	1.64	-109.79			[81]
a-4	83		208		298.43			[81]
a-5		-60	221	1.55	-187.36			[81]
a-6	86		259	1.66	215.17			[81]
b-1-1	147		174	1.76	218.65			[82]
b-1-2	123		154	-	-			[82]
b-1-3	118		136	1.68	156.38			[82]
b-1-4	97		136					[82]
b-2-1	66		139	1.63	93.35			[82]
b-2-2	55		147	1.66	574.73			[82]
b-3-1	68		147					[82]
b-3-1	98		129					[82]
c-1-1	92		158	1.70	401.85			[83]
c-1-2	80		148	1.60	700.69			[83]
c-2-1	64		198	1.50	141.38			[83]
c-3-1		-35	161	1.53	965.20			[83]
c-3-2		-38	141	1.45	1070.68			[83]
d-1	97		239	1.86	118.1			[84]
d-2	61		231	1.51	198.7			[84]
d-3	88		189	1.61	395.2			[84]
d-4		-43	179	1.71	771.3			[84]
d-5		-22	118	1.60	778.1			[84]
d-6	112		234	1.70	378.3			[84]
d-7	173		199	1.72	161.4			[84]
d-8	141		166	1.64	660.3			[84]

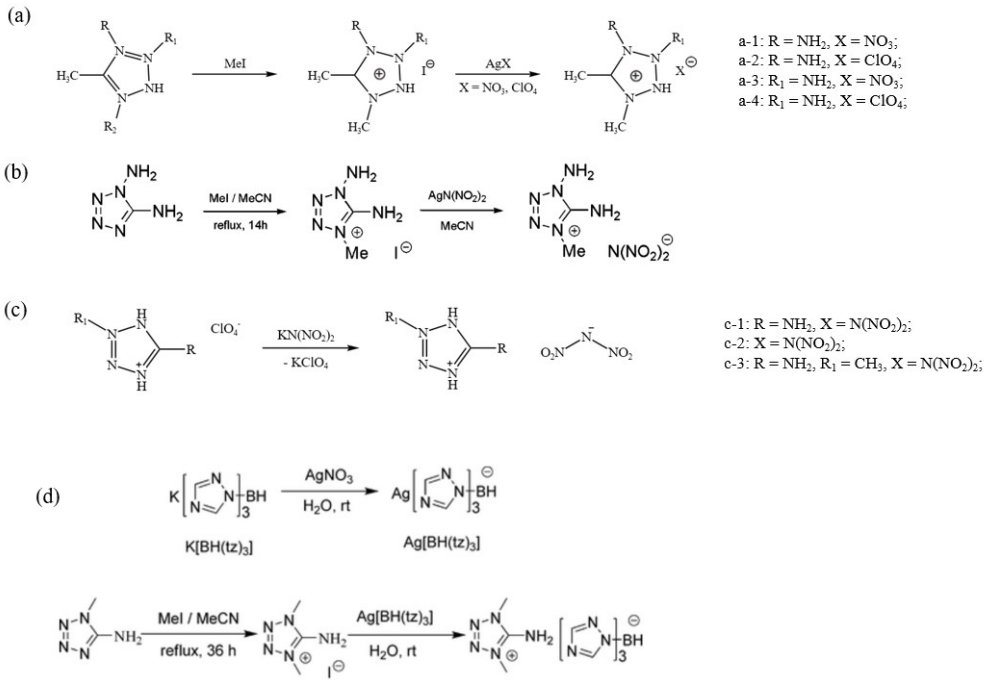

Figure S21. Molecular structure of tetrazolimidazole based energetic ionic liquids.

Table S15. The properties of some tetrazolimidazole based energetic ionic liquids.

EILs	T_m, ℃	T_g, ℃	T_d, ℃	ρ, g/cm^3	△H f,, kJ/mol	V_d, m/s	P_d, GPa	IS, J	FS, J	Ref.
a-1	-	-59	170	1.55	129.52					[81]
a-2	51		182	1.71	538.53					[81]
a-3	94		173	1.55	163.41					[81]
a-4	140		238	1.71	911.21					[81]
b	85		150						24	[85]
c-1	85		117	1.86	329	9429	38.4	2	20	[86]
c-2	70		110	1.82	367	9215	36.5	2	28	[86]
c-3	90		145	1.66	296	8548	29.0	5	64	[86]
d	11.8		81.7	12.4						[87]

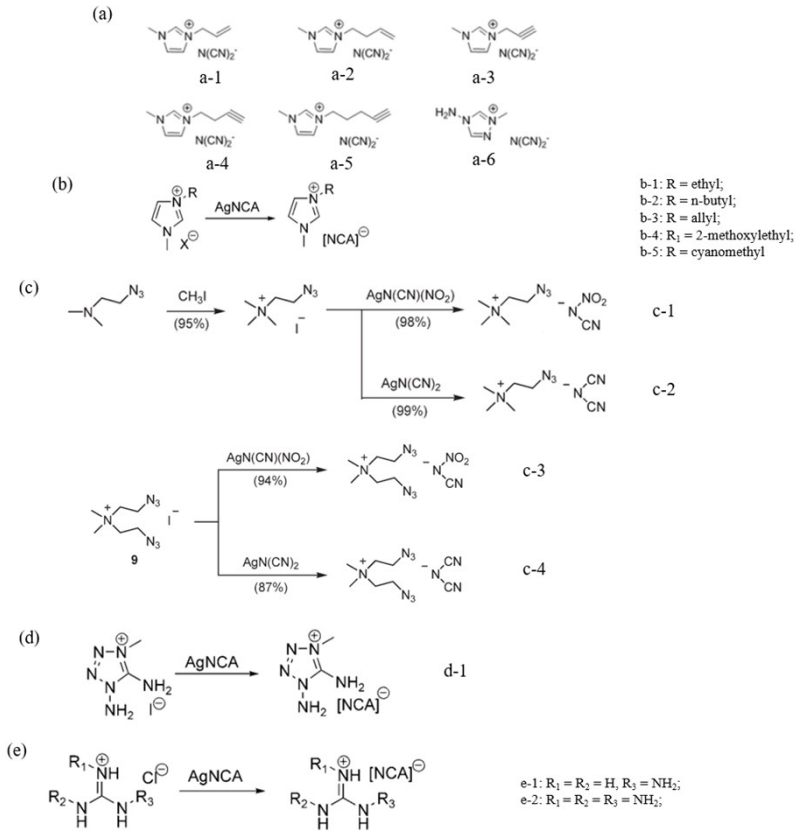

Figure S22. Molecular structure of tetrazolimidazole based energetic ionic liquids.

Table S16. The properties of some hypergolic ionic liquids.

EILs	T_g, ℃	T_d, ℃	ρ, g/cm^3	η,cP	△H f,, kJ/mol	△H_c, kJ/mol	ID, ms	I_{sp}	Ref.
a-1	-85	207		42			43		[88]
a-2	-90	210		27					[88]
a-3	-61	144		110			15		[88]
a-4		179							[88]
a-5		184							[88]
a-6	-66	143		92			31		[88]
b-1	-73	253	1.18	23	157.7		78	192.3	[89]
b-2	-90	256	1.13	57	128.5		81	184.6	[89]
b-3	-91	220	1.11	44	274.7		46	196.7	[89]
b-4	-82	266	1.21	54	44.3		65	187.0	[89]
b-5		203	1.47		368.9			203.2	[89]
c-1		245	1.24		380		8	218	[90]
c-2		235	1.15		518		20	202	[90]
c-3		222	1.32		752		226	231	[90]

c-4		222	1.21	894	16	231	[90]
d-1	-47	188	1.58	409		225.	[89]
e-1	91	223	1.53	138.2		212.2	[89]
e-2	74	209	1.59	322.8		227.0	[89]

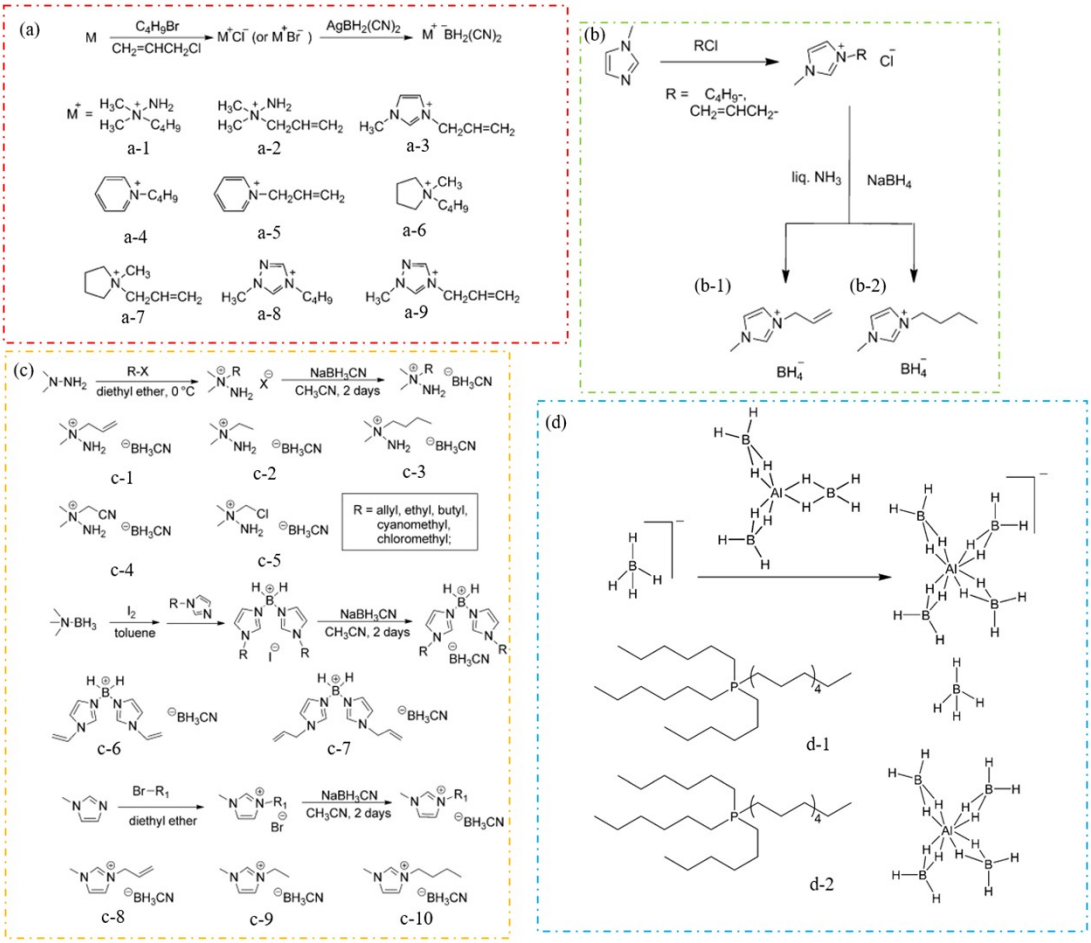

Figure S23. Molecular structure of HILs incorporating B–H-containing anions.

Table S17. The properties of some HILs incorporating B–H-containing anionss.

EILs	T_g, ℃	T_d, ℃	ρ, g/cm^3	η,cP	△H f,, kJ/mol	$\triangle H_c$, kJ/mol	ID, ms	I_{sp}	Ref.
a-1	<-80	222	0.91	39.4			6		[91]
a-2	<-80	189	0.93	35.0			4		[91]
a-3	<-80	266	0.99	12.4			8		[91]
a-4	<-80	252	0.96	19.8			18		[91]
a-5	<-80	203	1.00	13.5			6		[91]
a-6	<-80	303	0.92	22.3			26		[91]
a-7	<-80	259	0.94	16.6			8		[91]
a-8	<-80	220	0.99	29.9			32		[91]

a-9	<-80	217	1.03	21.0			6		[91]
b-1	<-60	93.3	0.90	113.8	118	-5653	3		[92]
b-2	<-60	99.9	0.91	486.6	39	-6539	38		[92]
c-1	-80	181	0.93	113	155	-5439	42	214	[93]
c-2	-17	205	0.92	242	40	-4931	103	208	[93]
c-3	-80	201	0.89	124	20	-6270	54	198	[93]
c-4		127	0.94		282	-4744		228	[93]
c-5		134	1.15		58	-4127		204	[93]
c-6	-37	174	0.89	523	573	-8605	41	219	[93]
c-7	-59	190	0.88	196	245	-9635	23	188	[93]
c-8	-80	242	0.96	28	337	-6122	8	211	[93]
c-9	-71	247	0.98	19	319	-5610	4	206	[93]
c-10	-80	267	0.97	102	191	-6941	24	195	[93]

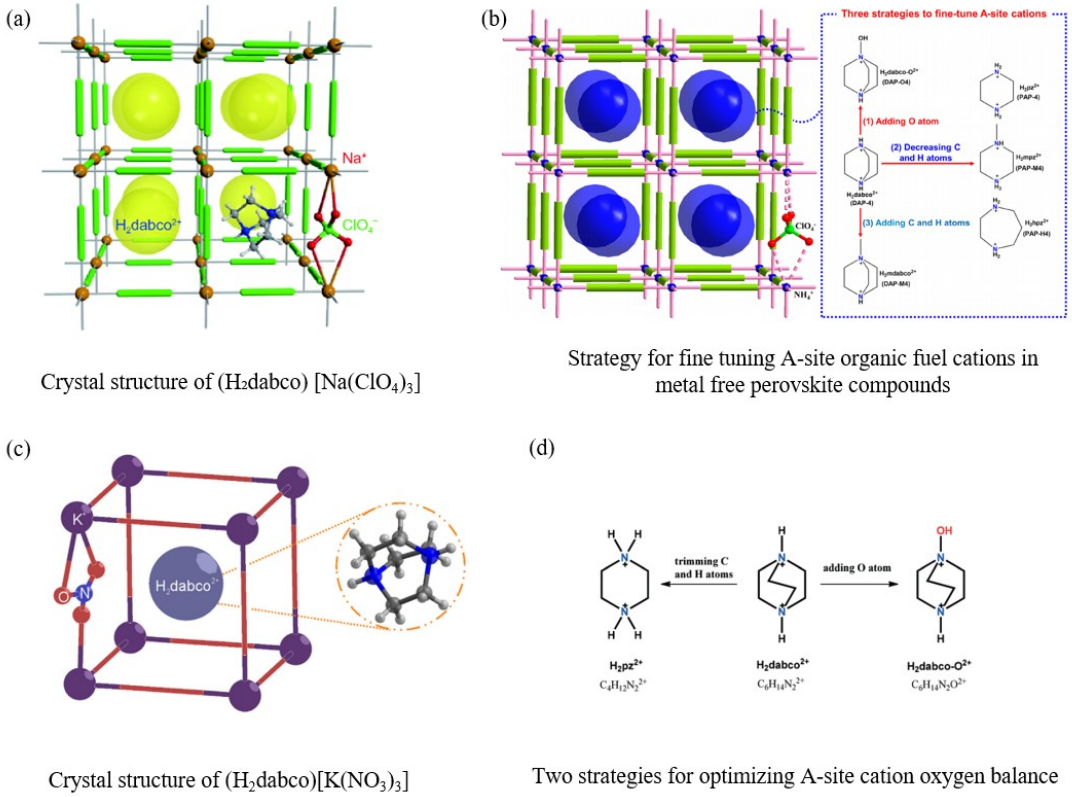

Crystal structure of (H_2dabco) [$Na(ClO_4)_3$]

Strategy for fine tuning A-site organic fuel cations in metal free perovskite compounds

Crystal structure of (H_2dabco)[$K(NO_3)_3$]

Two strategies for optimizing A-site cation oxygen balance

Figure S24. Perovskite-inspired energetic materials[94-97]. Copyright 2018, 2020, and 2022 Springer Nature, ACS, RSC, and KeAi.

Table S18. The properties of some HILs incorporating B–H-containing anionss.

Compounds	T_d, °C	T_p, °C	ρ, g/cm^3	△H f,, kJ/mol	Q, kJ/g	V_d, m/s	P_d, GPa	IS, J	FS, N	Isp, s	Ref.

DAP-1	344	361	2.02	1013.7	8.89	9306	48.3	17	36	-	[94]
DAP-2	364	377	2.04	247.3	7.09	9224	44.2	16	42	-	[94]
DAP-3	352	369	2.16	-	-	-	-	22	28	-	[94]
DAP-4	365	383	1.87	1904.2	10.38	9588	49.4	23	36	344	[94]
DAP-O4	352	-	1.85	436.0	6.21	8900	35.7			262	[95]
DAP-M4	364		1.78	839.1	4.99	8085	28.8			225	[95]
PAP-4	288		1.74	537.7	6.00	8629	32.4			264	[95]
PAP-M4	323		1.77	859.9	5.14	8311	30.3			241	[95]
PAP-H4	348		1.83	600.4	5.76	8756	34.3			255	[95]
PAP-5	342		2.50		4.88	8961	42.4				[98]
PAP-M5	307		2.37		5.42	8778	39.7				[98]
PAP-H5	328		2.37		5.36	8756	39.5				[98]
DAN-2	-	-	1.68	339.1	5.43	7566	23.4	29	>360		[96]
DAI-1	152		2.90	83.31	3.58	6438	30.79		<5		[99]
DAI-2	165		2.95	118.5	3.48	6331	30.88		<5		[99]
DAI-3	156		3.06						<5		[99]
DAI-4	155		2.79	36.9	3.41	6558	30.69		<5		[99]

DAP-1: (H_2dabco)[$Na(ClO_4)_3$], DAP-2: (H_2dabco) [$K(ClO_4)_3$], DAP-3: (H_2dabco) [$Rb(ClO_4)_3$], DAP-4: (H_2dabco) [$NH_4(ClO_4)_3$], DAP-O4: (H_2dabco-O^{2+}) [$NH_4(ClO_4)_3$], DAP-M4: (H_2mdabco) [$NH_4(ClO_4)_3$], PAP-4: (H_2pz) [$NH_4(ClO_4)_3$], PAP-M4: (H_2mpz) [$NH_4(ClO_4)_3$], PAP-H4: (H_2hpz) [$NH_4(ClO_4)_3$], PAP-5: (H_2pz) [$Ag(ClO_4)_3$], PAP-M5: (H_2mpz) [$Ag(ClO_4)_3$], PAP-H5: (H_2hpz) [$Ag(ClO_4)_3$], DAN-2: (H_2dabco)[$K(NO_3)_3$], DAI-1: (H_2dabco)[$Na(IO_4)_3$], DAI-2: (H_2dabco)[$K(IO_4)_3$], DAI-3: (H_2dabco)[$Rb(IO_4)_3$], DAI-4: (H_2dabco)[$NH_4(IO_4)_3$].

Energetic coordination compounds

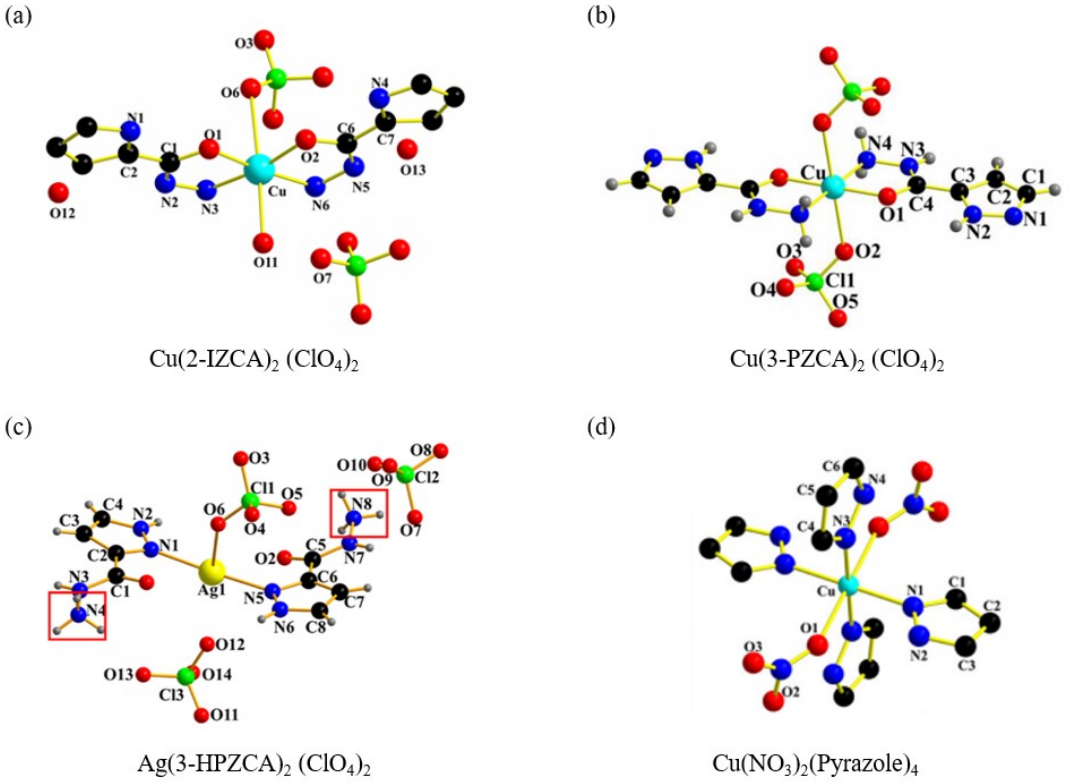

Figure S25. Molecular structure of some zero-dimensional ECCs [100-103] . Copyright 2023, 2024, and 2025 ACS and RSC.

Table S19. The properties of some zero-dimensional ECCs.

Compounds	T_d, ℃	ρ, g/cm^3	△H f,, kJ/mol	V_d, m/s	P_d, GPa	IS, J	FS, N	Ref.
$Cu(PRCA)_2(ClO_4)_2$	219	1.83		6300	16.4	7	16	[100]
$Cu(3\text{-}PZCA)_2(ClO4)_2$	190	1.96		7100	23.5	2	7	[101]
$Cu(2\text{-}IZCA)2(ClO4)_2$	225	1.94		7100	22.1	3	8	[101]
$Ag(3\text{-}HPZCA)_2(ClO_4)_3$	258	2.09		7600	28.5	13	40	[102]
$Cu(NO_3)_2(Pyz)_4$	208	1.61	88.1	6138	13.2	40	360	[103]
$Cu(NO_3)_2(CPyz)_4$	222	1.78	29.8	5780	15.3	40	360	[103]
$Cu(ClO_4)_2(Pyz)_4$	237	1.72	281.7	6215	16.8	14	192	[103]
$Cu(ClO_4)_2(CPyz)_4$	268	1.81	248.9	6190	17.8	10	168	[103]

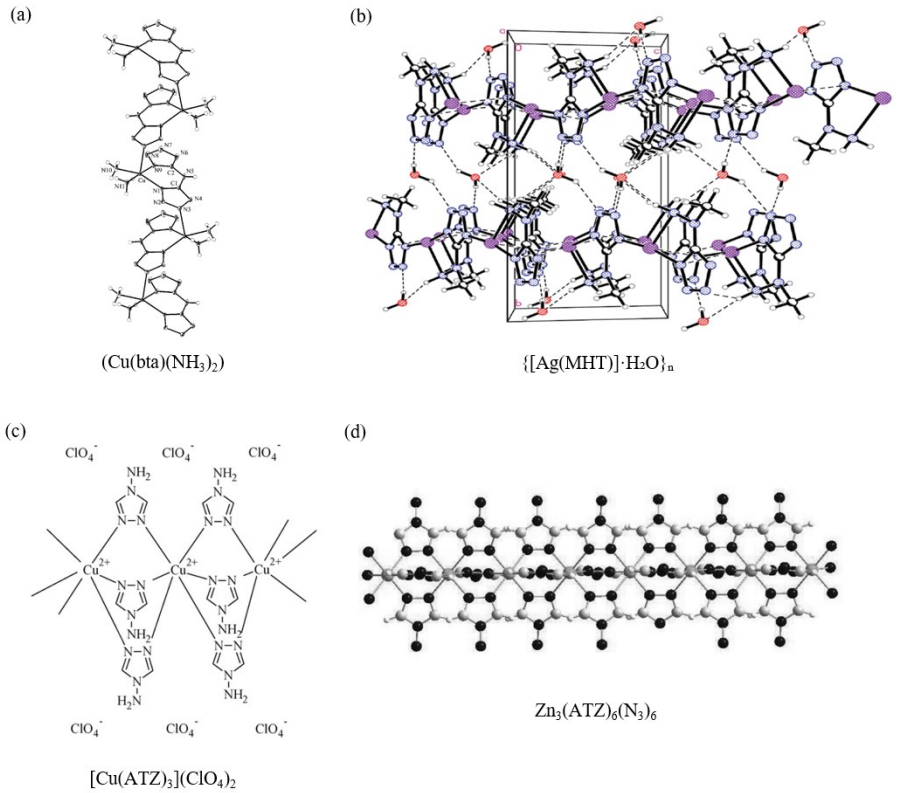

Figure S26. Molecular structure of some one-dimensional ECCs [104-107]. Copyright 2005, 2010, 2012, and 2013 ACS, Elsevier, and Wiley.

Table S20. The properties of some one-dimensional ECCs.

Compounds	T_d, ℃	ρ, g/cm^3	△H f,, kJ/mol	V_d, m/s	P_d, GPa	IS, J	FS, N	Ref.
$Cu(bta)(NH_3)_2·H_2O$	250	2.00	87.8			>40	>360	[104]
$[Ag(MHT)]·H_2O$	200	2.47	-263			>40		[105]
$[Cu(ATZ)_3](ClO_4)_2$	>250	1.4		6500		1	8.8	[106]
$Zn_3(ATZ)_6(N_3)_6$	137	1.82				>40		[107]
$Ni(N_2H_4)_5(ClO_4)_2$	220	1.98		9200	36.8			[108]
$Co(N_2H_4)_5(ClO_4)_2$	194	1.95		8225	31.7	0.5		[108]
$Ni(N_2H_4)_3(NO_3)_2$	-	2.16		7300	20.2			[108]

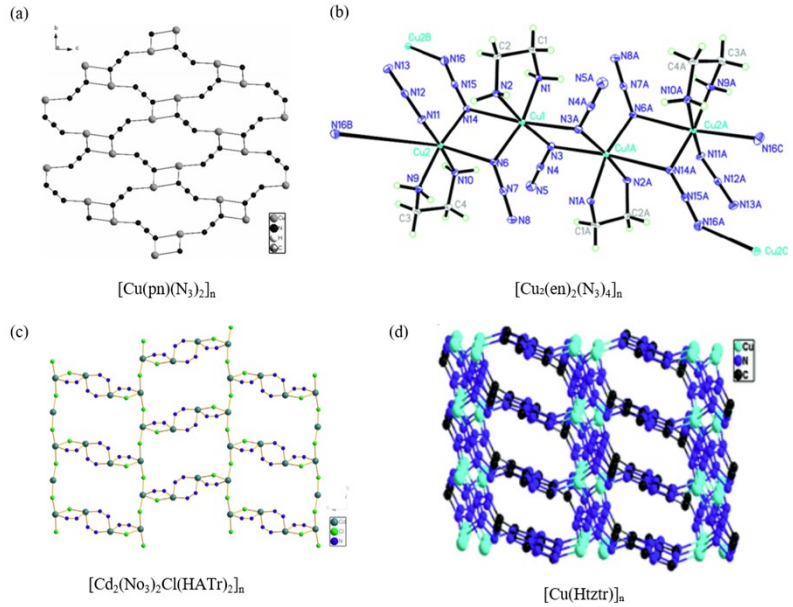

Figure S27. Molecular structure of some two-dimensional ECCs [109-112]. Copyright 2013 and 2015 Wiley, RSC and Elsevier.

Table S21. The properties of some two-dimensional ECCs.

Compounds	T_d, ℃	ρ, g/cm^3	△H f,, kJ/mol	V_d, m/s	P_d, GPa	IS, J	FS, N	Ref.
$Cu(pn)(N_3)_2$	215.7	1.76	-2320.76			2.55		[109]
$Cu_2(en)_2(N_3)_4$	201.8	1.93	-1330.34			7.84		[110]
$Cd_2(NO_3)_2Cl_2(HATr)_2$	224.85	2.47						[111]
Cu(Htztr)	200	2.03	93			>40		[112]

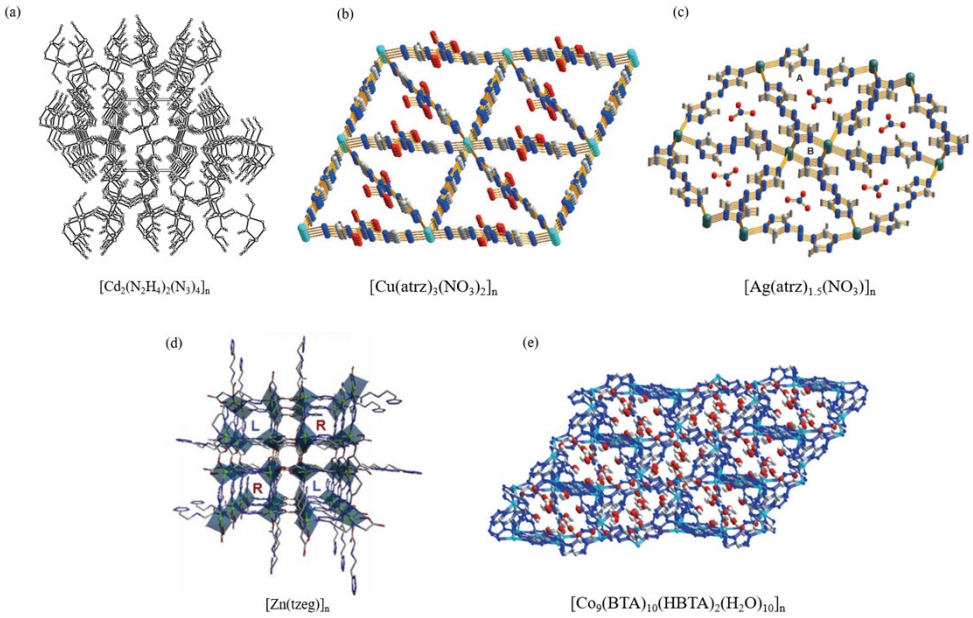

Figure S28. Molecular structure of some three-dimensional ECCs [113-116]. Copyright 2008, 2013,

and 2014 Elsevier, RSC and Wiley.

Table S22. The properties of some two-dimensional ECCs.

Compounds	T_d, ℃	ρ, g/cm^3	△H f,, kJ/mol	V_d, m/s	P_d, GPa	IS, J	FS, N	Ref.
$Cd_2(N_2H_4)_2(N_3)_4$	151	2.64				>40		[113]
Zn(tzeg)	425	1.88	-491.78					[114]
$Cu(atrz)_3(NO_3)_2$	243	1.68		9160	35.68	22.5		[115]
$Ag(atrz)_{1.5}(NO_3)$	257	2.16		7773	29.70	30		[115]
$Co_9(BTA)_{10}(HBTA)_2(H_2O)_{10}$	253	1.71	859.66	8657	32.18	27	>360	[116]

Metal and Non-metal Fuel

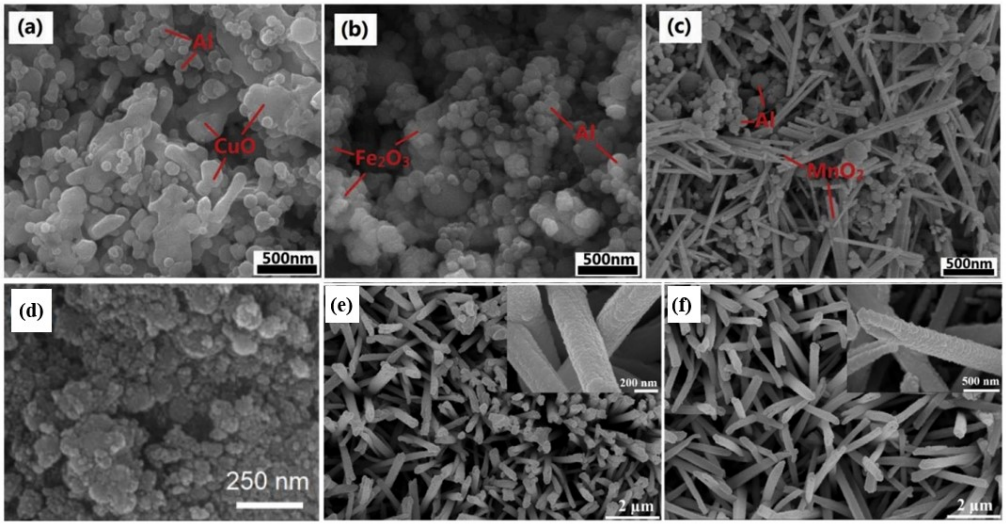

Figure S29. The SEM images of thermites (a) Al/CuO nanothermite, (b) Al/Fe_2O_3 nanothermite, (c) Al/MnO_2 nanothe[117], Copyright 2020 Elsevier. (d) Field emission scanning electron microscopy (FESEM) imageof Al/Fe_2O_3 nEMs by soft template self-assembly with sol-gel process [118], Copyright 2015 Elsevier (e) CuO nanorod/Al MICs and (f) CuO nanotube/Al MICs[119], Copyright 2018 Elsevier.

Table S23. Thermo-physical properties of various thermite reactions [120].

Reactants		Adiabatic reaction temperature (without phase changes)[K]	Gas production		Heat of reaction	
Constituents	Density[g/cm^3]		Moles of gas/100 g	g of gas/g	[kJ/g]	[kJ/cm^3]
2Al+Cr_2O_3	4.190	2789	0	0	2.6	10.9
2Al+3CuO	5.109	5718	0.5400	0.3431	4.1	20.8

$2Al+3Cu_2O$	5.280	4132	0.1221	0.0776	2.4	12.7
$2Al+Fe_2O_3$	4.175	4382	0.1404	0.0784	4.0	16.5
$8Al+3Fe_3O_4$	4.264	4075	0.0549	0.0307	3.7	15.7
$4Al+3MnO_2$	4.014	4829	0.8136	0.4470	4.8	19.5
$2Al+ MoO_2$	3.808	5574	0.2425	0.2473	4.7	17.9
$4Al+ 3SnO_2$	5.356	5019	0.2928	0.3476	2.9	15.4
$10Al+3V_2O_5$	3.107	3953	0.0699	0.0356	4.6	14.2
$4Al+3WO_2$	8.085	4176	0.0662	0.0675	2.1	16.9
$2Al+WO_3$	5.458	5544	0.1434	0.1463	2.9	15.9

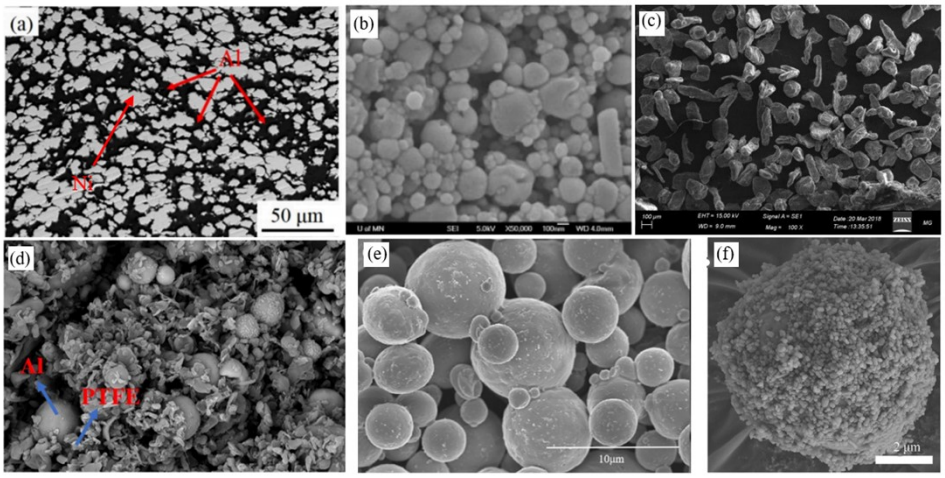

Figure S30. The SEM images of thermites (a) Ni-Al energetic material[121], Copyright 2024 ACS. (b) $KMnO_4$-Al energetic material[122], Copyright 2005 Wiley (c) Mg-Al energetic material[123], Copyright 2024 IOP Publishing (d) Al/PTFE energetic material[124], Copyright 2023 Elsevier (e) μAl@2.5% PFPE energetic material[125], Copyright 2023 Elsevier (f) the PTFE-coated Al particle of core-shell structured PTFE/Al[126], Copyright 2022 Elsevier.

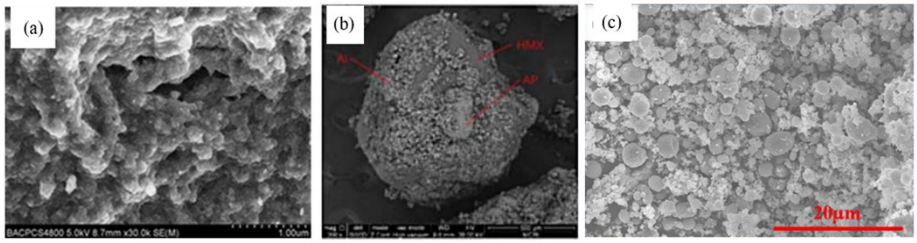

Figure S31. The SEM images of thermites (a) AP/Al/Fe_2O_3 energetic material[127], Copyright 2014 Springer (b) Al/AP/HMX energetic material[128], Copyright 2024 Wiley (c) Al/Ti/CuO-P energetic material[129], Copyright 2023 Elsevier.

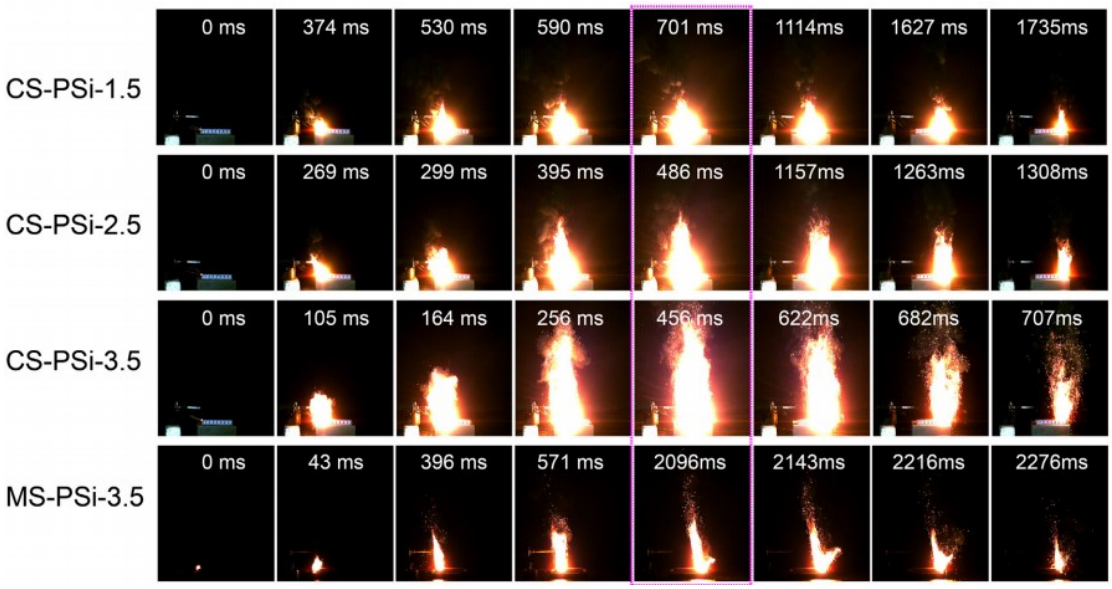

Figure S32. High-speed photographic sequences of the combustion processes of CS-PSi-1.5, CS-PSi-2.5, CS-PSi-3.5, and MS-PSi-3.5 composites [130], Copyright 2023 Elsevier.

Oxidisers

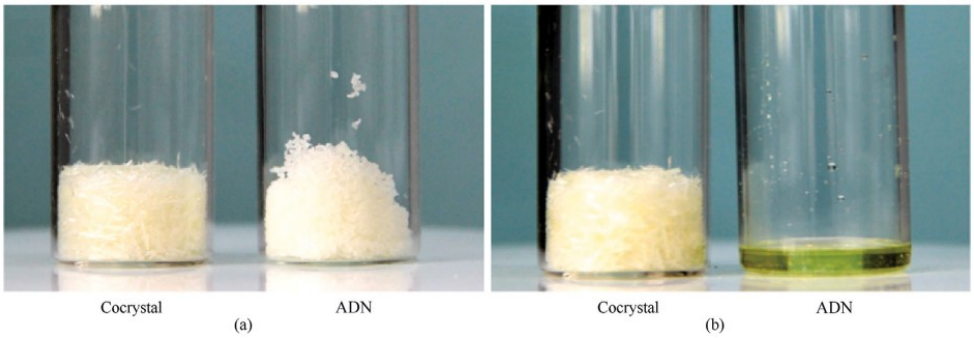

Figure S33. Status of ADN/18C6 cocrystal and pure ADN (a) before and (b) after hygroscopic test.

Binders

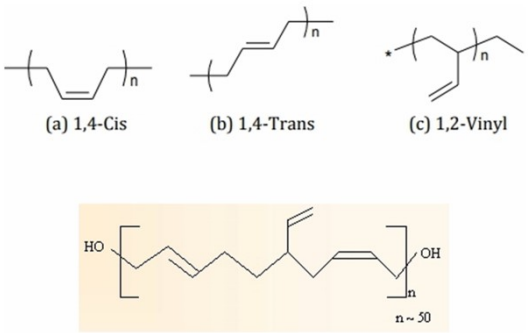

Figure S34. Microstructure of hydroxyl-terminated polybutadiene [131], Copyright 2022 Wiley.

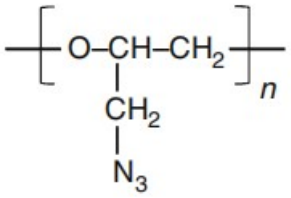

Figure S35. Structure of the monomer of GAP[132], Copyright 2019 MDPI.

Curing Agent

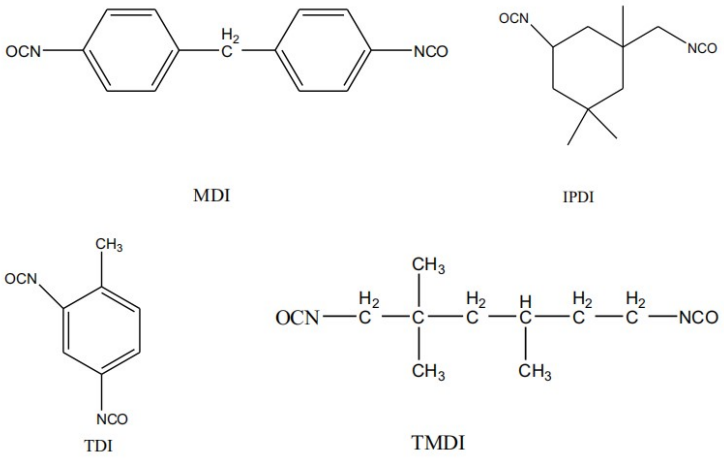

Figure S36. The chemical structure of various diisocyanates compounds [133], Copyright 2024 Taylor & Francis.

Macroscopic Structuring of Energetic Materials

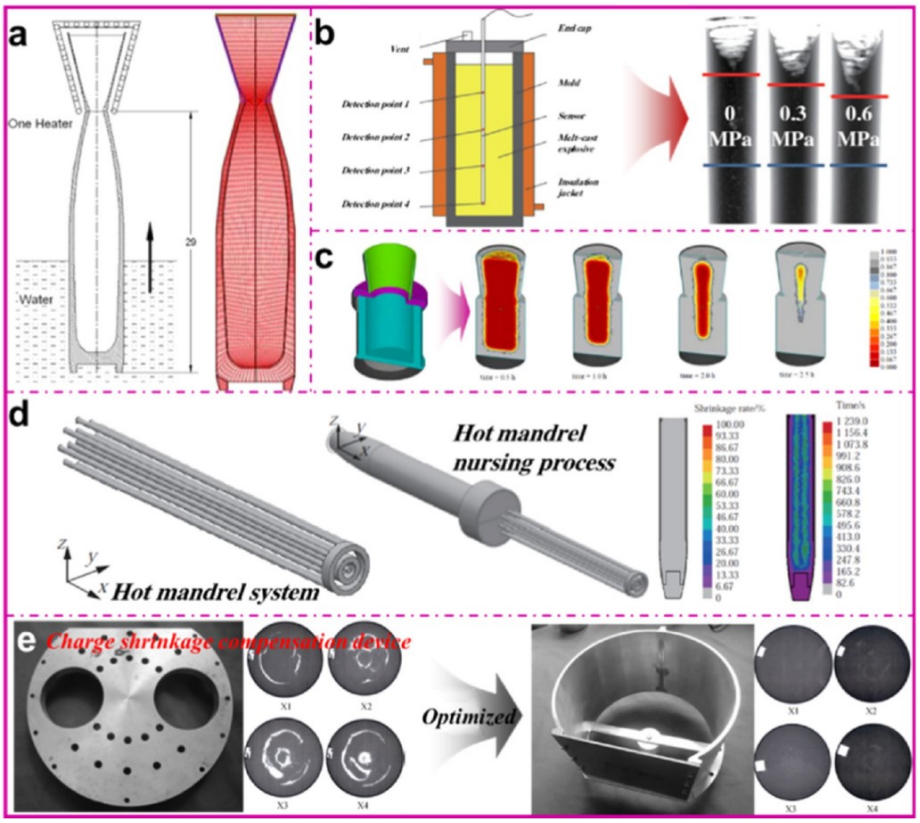

Figure S37. High-density melt-cast charge technology: (a) solidification in a water bath,(b) pressurized treatment, (c) riser insulation, (d) hot mandrel treatment, and (e) optimization of feeding setup [134], Copyright 2023 ACS.

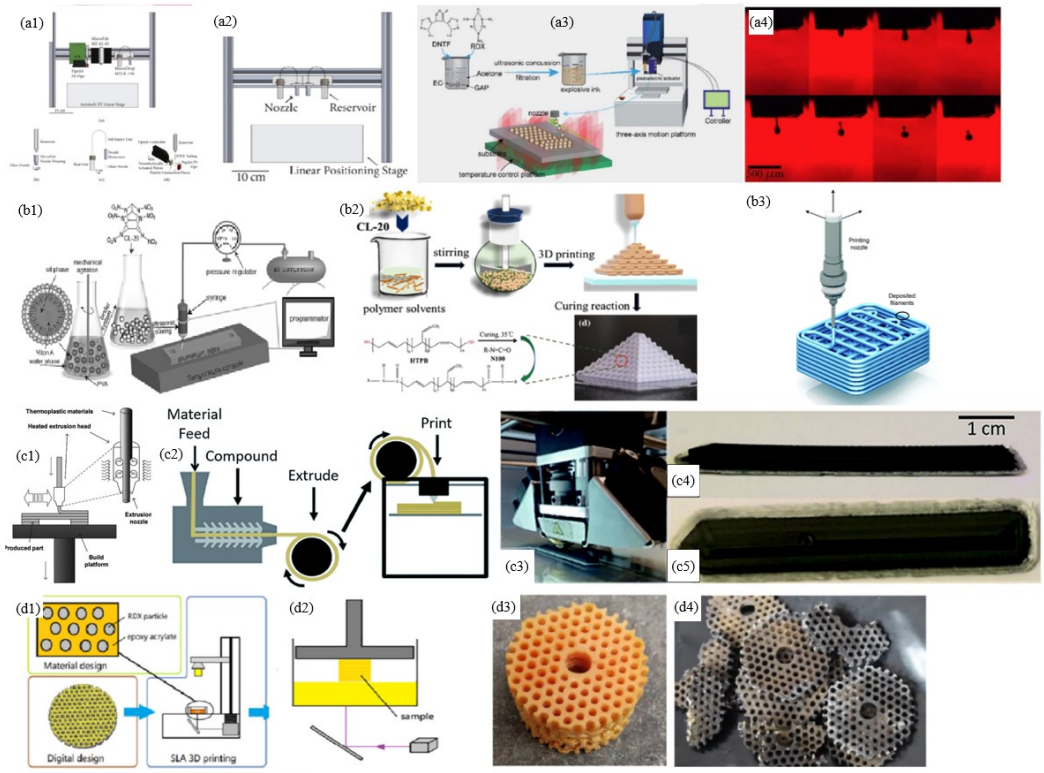

Figure S38. (a1) Three printing systems of Inkjet printing . (a2) Printing system with two piezoelectric inkjet nozzles. (a3) Printing system with three-axis platform and piezoelectric nozzle. (a4) Nano-aluminum droplets. (b1) Schematic illustration of the preparation of printed inks consisting of an emulsion binder and CL-20 explosives. (b2) Schematic illustration of 3D printing (DIW) of the CL-20 based explosives. (b3) Schematic illustration of DIW. (c1) the detail view of the extrusion assembly equipment and the printing stage. (c2) SLA schematic illustration of the manufacturing process. (c3) The completed sample side view. (c4) The completed print sample side view. (d1, d2) Diagram of the SLA process (d3) Photos of 3D-printed MPD propellant stack and (d4) remaining propellants after 30 mm gun test[135, 136], Copyright 2022 KeAi and Chinese Society of Metals.

Uncategorized References

[1] C. Li, H. Li, K. Xu, High-substitute nitrochitosan used as energetic materials: Preparation and detonation properties, Carbohydr. Polym. 237 (2020) 116176.

[2] J. Dong, Q. Yan, P. Liu, et al., The correlations among detonation velocity, heat of combustion, thermal stability and decomposition kinetics of nitric esters, J. Therm. Anal. Calorim. 131 (2017) 1391-1403.

[3] W. E. Bachmann, J. C. Sheehan, A new method of preparing the high explosive RDX, J. Am. Chem. Soc. 71 (1949) 1842-1845.

[4] K. F. Grebenkin, Comparative Analysis of Physical Mechanisms of Detonation Initiation in HMX and in aLow-SensitiveExplosive (TATB), Combust. Explos. Shock Waves 45 (2009) 78-87.

[5] T.A. Nielsen, A.P. Chafin, S.L. Christian, et al., Synthesis of polyazapolycyclic caged polynitramines, Tetrahedron 54 (1998) 11793-11812.

[6] N. Şen, J. F. Pons, G. Kurtay, et al., New explosive materials through covalent and non-covalent synthesis: Investigation of explosive properties of trinitrotoluene: Acridine and picric acid: Acridine, J. Mol. Struct. 1292 (2023) 136080.

[7] C. Li, M. Liu, T. Li, et al., Fluorine Added to Lead the Way to Future Energetic Materials: 3,5-difluoro-2,4,6-trinitroaniline, J. Energ. Mater. 42 (2022) 706-715.

[8] X. Liao, X. Ju, F. Zhao, et al., Substituent Effects on Thermodynamic and Detonation Properties of Polynitrobenzenes, Propellants Explos. Pyrotech. 35 (2010) 567-571.

[9] H. Gao, Q. Zhang, J. Shreeve, Fused heterocycle-based energetic materials (2012–2019), J. Mater. Chem. A 8 (2020) 4193-4216.

[10] D. Guo, S. Zybin, W. Goddard, et al., Enhancing the Detonation Properties of Liquid Nitromethane by Adding Nitro-Rich Molecule Nitryl Cyanide, J. Phys. Chem. A 124 (2020) 9787-9794.

[11] Z. Yin, W. Huang, Y. Dong, et al., From Tetranitromethane to Gem-Dinitro-Bridged Nitrogen-Rich Heterocyclic Compound: Achieving High Heat of Detonation, J. Org. Chem. 88 (2023) 14004-14011.

[12] H. Gao, J. M. Shreeve, Recent progress in taming FOX-7 (1,1-diamino-2,2dinitroethene), Rsc Adv. 6 (2016) 56271-56277.

[13] I. V. Fedyanin, K. A. Lyssenko, New hydrogen-bond-aided supramolecular synthon: a case study of 2,4,6-trinitroaniline, CrystEngComm 15 (2013) 10086–10093.

[14] A. V. Kimmel, P. V. Sushko, A. L. Shluger, et al., Effect of molecular and lattice structure on hydrogen transfer in molecular crystals of diamino-dinitroethylene and triamino-trinitrobenzene, J. Phys. Chem. A 112 (2008) 4496–4500.

[15] Z. Zhang, Y. Si, T. Yu, et al., Extra contribution to the crystal stability of insensitive explosive TATB: The cooperativity of intermolecular interactions, Def. Technol. 25 (2023) 88-98.

[16] W. Zhu, H. Xiao, Ab Initio Study of Energetic Solids: Cupric Azide, Mercuric Azide, and Lead Azide, J. Phys. Chem. B 110 (2006) 18196-18203.

[17] P. Sivaguru, Y. Ning, X. Bi, New Strategies for the Synthesis of Aliphatic Azides, Chem. Rev. 121 (2021) 4253-4307.

[18] Q. Sun, P. Wang, Q. Lin, et al., All-nitrogen ion-based compounds as energetic oxidizers: a theoretical study on [N5+][NO3−], [N5+][N(NO2)2−], [NO2+][N5−] and NO2–N3, New J. Chem. 44 (2020) 11188-11195.

[19] Y. Xu, P. Wang, Q. Lin, et al., Density functional theory studies on two novel poly-nitrogen compounds: N5+N3− and N5+N5−, J. Phys. Org. Chem 34 (2020) e4135.

[20] K. O. Christe, W. W. Wilson, J. A. Sheehy, et al., N5+: A Novel Homoleptic Polynitrogen Ion as a High Energy Density Material, Angew. Chem. Int. Ed. 38 (1999) 2004-2009.

[21] A. Vij, W. W. Wilson, V. Vij V, et al., Polynitrogen Chemistry. Synthesis, Characterization, and Crystal Structure of Surprisingly Stable Fluoroantimonate Salts

of N5+, J. Am. Chem. Soc. 123 (2001) 6308-6313.
[22] C. Yang, C. Zhang, Z. Zheng, et al., Synthesis and Characterization of cyclo-Pentazolate Salts of NH(4)(+), NH(3)OH(+), N(2)H(5)(+), C(NH(2))(3)(+), and N(CH(3))(4)(), J. Am. Chem. Soc. 140 (2018) 16488-16494.
[23] Y. Xu, L. Tian, D. Li, et al., A series of energetic cyclo-pentazolate salts: rapid synthesis, characterization, and promising performance, J. Mater. Chem. A 7 (2019) 12468-12479.
[24] X. Wang, Z. Dong, R. Yang, et al., Syntheses and Characterization of two cyclo-pentazolate salts, Z. Anorg. Allg. Chem. 647 (2021) 681-685.
[25] Y. Xu, Q. Wang, C. Shen, et al., A series of energetic metal pentazolate hydrates, Nature 549 (2017) 78-81.
[26] C. Yang, L. Chen, W. Wu, et al., Investigating the stabilizing forces of pentazolate salts., ACS Appl. Energy Mater. 4 (2020) 146-153.
[27] Y. Xu, P. Wang, Q. Lin, et al., A carbon-free inorganic–metal complex consisting of an all-nitrogen pentazole anion, a Zn(ii) cation and H2O, Dalton. Trans. 46 (2017) 14088-14093.
[28] W. Hu, H. Yang, J. Chen, et al., Nonmetallic Pentazole Salts Based on Furazan or 4-Nitropyrazole for Enhancing Density and Stability, Cryst. Growth Des. 21 (2021) 2690-2698.
[29] F. Jiao, C. Zhang, Origin of the considerably high thermal stability of cyclo-N5− containing salts at ambient conditions, CrystEngComm 21 (2019) 3592-3604.
[30] T. M. Klapötke, M. Stein, J. Stierstorfer, Salts of 1H-Tetrazole – Synthesis, Characterization and Properties, Z. Anorg. Allg. Chem. 634 (2008) 1711-1723.
[31] P. Ma, X. Xu, R. Zhang, et al., Synthesis, thermal hazard analysis and density functional theory study of nitroimidazoles, Thermochim. Acta 707 (2022) 179097.
[32] J. R. Cho, K. J. Kim, S. G. Cho, et al., Synthesis and characterization of 1-methyl-2,4,5-trinitroimidazole (MTNI), J. Heterocycl. Chem. 39 (2009) 141-147.
[33] T. M. Klapötke, C. M. Sabaté, J. Stierstorfer, Neutral 5-nitrotetrazoles: easy initiation with low pollution, New J. Chem. 33 (2009) 136-147.
[34] Y. Kang, Y. Dong, Y. Liu, et al., Halogen bonding (C-F···X) and its effect on creating ideal insensitive energetic materials, Chem. Eng. J. 440 (2022) 135969.
[35] M. Thomas, Klapötke, Sabaté Carles Miró, Nitrogen-Rich Tetrazolium Azotetrazolate Salts: A New Family of Insensitive Energetic Materials, Chem. Mater. 20 (2008) 1750–1763.
[36] P. Yin, J. Zhang, D. A. Parrish, et al., Energetic fused triazoles – a promising C–N fused heterocyclic cation, J. Mater. Chem. A 3 (2015) 8606-8612.
[37] J. Zhang, D. A. Parrish, J. M. Shreeve, Thermally stable 3,6-dinitropyrazolo[4,3-c]pyrazole-based energetic materials, Chem. Asian. J. 9 (2014) 2953-60.
[38] Y. Tang, C. He, G. H. Imler, et al., Dinitromethyl-3(5)-1,2,4-oxadiazole Derivatives from Controllable Cyclization Strategies, Chem. Eur. J. 23 (2017) 16401-16407.
[39] D. E. Chavez, M. C. Schulze, D. A. Parrish, Synthesis and Characterization of N 3 -(2,2,2-Trinitroethyl)-1,2,4-Oxadiazole-3,5-Diamine, Chem. Heterocycl. Comp. 53 (2017) 737-739.
[40] Y. Tang, J. Zhang, L. A. Mitchell, et al., Taming of 3,4-Di(nitramino)furazan, J. Am. Chem. Soc. 137 (2015) 15984-15987.
[41] J. Ma, A. K. Chinnam, G. Cheng, et al., 1,3,4-Oxadiazole Bridges: A Strategy to Improve Energetics at the Molecular Level, Angew. Chem. Int. Ed. 60 (2021) 5497-5504.
[42] W. Cao, W. Dong, Z. Lu, et al., Construction of Coplanar Bicyclic Backbones for 1,2,4-Triazole-1,2,4-Oxadiazole-Derived Energetic Materials, Chemistry 27 (2021) 13807-13818.
[43] Q. Xue, F. Bi, J. Zhang, et al., A Family of Energetic Materials Based on 1,2,4-Oxadiazole and 1,2,5-Oxadiazole Backbones With Low Insensitivity and Good Detonation Performance, Front. Chem. 7 (2019) 942-951.

[44] T. Zhu, C. Li, J. Tang, et al., [5,6,5]-Tricyclic Energetic Compounds with Piperazine, Triazole, and 1,2,5-Oxadiazole Rings in Framework, Cryst. Growth Des. 24 (2024) 8847-8854.
[45] C. Ma, Y. Pan, J. Jiang, et al., Synthesis and thermal behavior of a fused, tricyclic pyridine-based energetic material: 4-amino-5-nitro-[1,2,5]oxadiazolo[3,4-e]tetra-zolo[1,5-a]pyridine-3-oxide, New J. Chem. 42 (2018) 11259-11263.
[46] Q. Wang, C. Lei, H. Yang, et al., One-step synthesis of polynitropyridine-based thermostable and low sensitive energetic materials, Energetic Mater. Front. 3 (2022) 68-73.
[47] C. Li, T. Zhu, C. Wang, et al., Advanced ultra heat-resistant explosives with multiple heterocyclic skeletons of hydrogen bond network, J. Mater. Chem. A 12 (2024) 24188-24194.
[48] H. Liu, H. Du, G. Wang, et al., Theoretical studies on the structures, densities, detonation properties and pyrolysis mechanism of energetic compounds containing pyridine ring, Struct. Chem. 23 (2011) 479-486.
[49] A. Maan, V. D. Ghule., S. Dharavath, Computational Evaluation of Polycyclic Bis-Oxadiazolo-Pyrazine Backbone in Designing Potential Energetic Materials, Polycycl. Aromat. Comp. 43 (2022) 6717-6729.
[50] J. Feng, J. Sun, L. Yang, et al., 3,7-Dinitroimidazo[1,2-b]pyridazine-6,8-diamine: A promising building block for advanced heat-resistant and low-sensitivity energetic materials, Energetic Mater. Front. 5 (2024) 1-7.
[51] X. Song, J. Li, H. Hou, et al., Extensive theoretical studies of a new energetic material: tetrazino-tetrazine-tetraoxide (TTTO), J. Comput. Chem. 30 (2009) 1816-1820.
[52] Y. Cao, Z. Cai, J. Shi, et al., A heat-resistant and insensitive energetic material based on the pyrazolo-triazine framework, Energetic Mater. Front. 3 (2022) 26-31.
[53] L. Hu, C. He, G. Zhao, et al., Selecting Suitable Substituents for Energetic Materials Based on a Fused Triazolo-[1,2,4,5]tetrazine Ring, ACS Appl. Energy Mater. 3 (2020) 5510-5516.
[54] I. Sedgi, S. Kozuch, Quantum tunneling instability of the mythical hexazine and pentazine, Chem. Commun. 60 (2024) 2038-2041.
[55] J. Zhang, H. Xiao, Computational studies on the infrared vibrational spectra, thermodynamic properties, detonation properties, and pyrolysis mechanism of octanitrocubane, J. Chem. Phys. 116 (2002) 10674-10683.
[56] Y. Bayat, G. Taheripouya, V. Zeynali, et al., Methods and strategies to achieve hexanitrohexaazaisowurtzitane (HNIW or CL-20): a comprehensive overview, J. Energ. Mater. 43 (2023) 62-96.
[57] X. Zeng, N. Li, Q. Jiao, Carbon-free energetic materials: computational study on nitro-substituted BN-cage molecules with high heat of detonation and stability, RSC Adv. 8 (2018) 14654-14662.
[58] Y. Ling, P. Zhang, L. Sun, et al., Efficient Synthesis of 2,2,4,4,6,6-Hexanitroadamantane under Mild Conditions, Synthesis 46 (2014) 2225-2233.
[59] T. M. Klapötke, B. Krumm, A. Widera, Synthesis and Properties of Tetranitro-Substituted Adamantane Derivatives, ChemPlusChem 83 (2018) 61-69.
[60] L. Zhu, Q. Zhou, W. Wang, et al., Synthesis and characterization of a new cage-like energetic compound 3,7-dinitrato-9-nitro-9-azanoradamantane, Energetic Mater. Front. (2024).
[61] J. Zhang, T. Hou, L. Zhang, et al., 2,4,4,6,8,8-Hexanitro-2,6-diazaadamantane: A High-Energy Density Compound with High Stability, Org. Lett. 20 (2018) 7172-7176.
[62] D. Chen, H. Xiong, H. Yang, et al., Nitropyrazole based tricyclic nitrogen-rich cation salts: A new class of promising insensitive energetic materials, FirePhysChem 1 (2021) 71-75.
[63] P. Bhatia, P. Das, D. Kumar, Engaging Two Anions with Single Cation in Energetic Salts: Approach for Optimization of Oxygen Balance in Energetic Materials, ACS Appl. Mater. Interfaces 16 (2024) 64846-64857.
[64] B.C. Tappan, C.D. Incarvito, A.L. Rheingold, et al., Thermal

decomposition of energetic materials 79: thermal, vibrational, and X-ray structural characterization of metal salts of mono-and di-anionic 5-nitraminotetrazole, Thermochim. Acta 384 (2002) 113-120.

[65] P. Yin, L. A. Mitchell, D. A. Parrish, et al., Comparative Study of Various Pyrazole-based Anions: A Promising Family of Ionic Derivatives as Insensitive Energetic Materials, Chem. Asian J. 12 (2017) 378-384.

[66] Z. Zhang, J. Zhang, 1-Amine-1,2,3-triazolium salts with oxidizing anions: A new family of energetic materials with good performance, J. Mol. Struct. 1158 (2018) 88-95.

[67] P. Yin, J. M. Shreeve, From N-Nitro to N-Nitroamino: Preparation of High-Performance Energetic Materials by Introducing Nitrogen-Containing Ions, Angew. Chem. Int. Ed. 54 (2015) 14513-14517.

[68] P. Bhatia, P. Das, A. Bijlwan, et al., Systematic Synthesis of Thermally Stable Zwitterionic Energetic Materials Based on 4-Hydroxy-3,5-dinitropyrazole, Org. Lett. 26 (2024) 9781-9786.

[69] X. Miao, J. Yu, Y. Li, et al., Constructing Nitrogen-Rich Fused [5,6,5]-Tricyclic Frameworks Through Rearrangement: Heat-Resistant Zwitterionic Salt Energetic Materials, Org. Lett. 26 (2024) 10085-10089.

[70] P. Kumar, N. Kumar, V. D. Ghule, et al., Zwitterionic fused pyrazolo-triazole based high performing energetic materials, Chem. Commun. 60 (2024) 1646-1649.

[71] R. Lv, L. Jiang, J. Wang, et al., A zwitterionic fused-ring framework as a new platform for heat-resistant energetic materials, J. Mater. Chem. A 12 (2024) 10050-10058.

[72] T. Liu, S. Liao, S. Song, et al., Combination of gem-dinitromethyl functionality and a 5-amino-1,3,4-oxadiazole framework for zwitterionic energetic materials, Chem. Commun. 56 (2020) 209-212.

[73] Z. Wang, Q. Lai, N. Ding, et al., Construction of zwitterionic 3D hydrogen-bonded networks: Exploring the upper-limit of thermal stability in ternary CHN-based energetic materials, Chem. Eng. J. 474 (2023) 145512.

[74] A. R. Katritzky, S. Singh, K. Kirichenko, et al., 1-butyl-3-methylimidazolium 3,5-dinitro-1,2,4-triazolate: a novel ionic liquid containing a rigid, planar energetic anion, Chem. Commun. (Camb) 7 (2005) 868-70.

[75] C. Ye, J. C. Xiao, B. Twamley, et al., Energetic salts of azotetrazolate, iminobis(5-tetrazolate) and 5, 5'-bis(tetrazolate), Chem. Commun. (Camb) 21 (2005) 2750-2752.

[76] S. Schneider, T. Hawkins, M. Rosander, et al., Liquid azide salts and their reactions with common oxidizers IRFNA and N2O4, Inorg. Chem. 47 (2008).

[77] A. R. Katritzky, H. Yang, D. Zhang, et al., Strategies toward the design of energetic ionic liquids: nitro- and nitrile-substituted N,N′-dialkylimidazolium salts, New J. Chem. 30 (2006) 349–358.

[78] M. Smiglak, C. C. Hines, T. B. Wilson, et al., Ionic liquids based on azolate anions, Chemistry 16 (2010) 1572-1584.

[79] R. Wang, H. Gao, C. Ye, et al., Strategies toward syntheses of triazolyl-or triazolium-functionalized unsymmetrical energetic salts., Chem. Mater. 19 (2007).

[80] L. He, G. H. Tao, D. A. Parrish, et al., Liquid dinitromethanide salts, Inorg. Chem. 50 (2011) 679-685.

[81] H. Xue, S. W. Arritt, B. Twamley, et al., Energetic salts from N-aminoazoles., Inorg. Chem. 43 (2004) 7972-7977.

[82] H. Xue, Y. Gao, B. Twamley, et al., New Energetic Salts Based on Nitrogen-Containing Heterocycles, Chem. Mater. 17 (2005) 191-198.

[83] H. Xue, Y. Gao, B. Twamley, et al., Energetic azolium azolate salts, Inorg. Chem. 44 (2005) 5068-5072.

[84] H. Xue, B. Twamley, J. M. Shreeve, Energetic salts of substituted 1,2,4-triazolium and tetrazolium 3,5-dinitro-1,2,4-triazolates, J. Mater. Chem. 15 (2005) 3459–3465.

[85] T. M. Klapötke, P. Mayer, A. Schulz, et al., 1, 5-Diamino-4-methyltetrazolium Dinitramide. , J. Am. Chem. Soc. 127 (2005) 2032-2033.

[86] T. M. Klapotke, J. Stierstorfer, Azidoformamidinium and 5-aminotetrazolium dinitramide-two highly energetic isomers with a balanced oxygen content, Dalton. Trans. (2009) 643-653.
[87] Z. Zeng, B. Twamley, J. N. M. Shreeve, Structure and properties of substituted imidazolium, triazolium, and tetrazolium poly (1, 2, 4-triazolyl) borate salts, Organometallics 26 (2007) 1782-1787.
[88] T. Schneider, T. Hawkins, M. Rosander, et al., Ionic liquids as hypergolic fuels, Energy Fuels 22 (2008) 2871-2872.
[89] L. He, G. Tao, D. A. Parrish, et al., Nitrocyanamide-based ionic liquids and their potential applications as hypergolic fuels, Chemistry 16 (2010) 5736-5743.
[90] Y. Joo, H. Gao, Y. Zhang, et al., Inorganic or organic azide-containing hypergolic ionic liquids, Inorg. Chem. 49 (2010) 3282-3288.
[91] Y. Zhang, J. M. Shreeve, Dicyanoborate-based ionic liquids as hypergolic fluids, Angew. Chem. Int. Ed. 50 (2011) 935-937.
[92] S. Li, H. Gao, J. M. Shreeve, Borohydride ionic liquids and borane/ionic-liquid solutions as hypergolic fuels with superior low ignition-delay times, Angew. Chem. Int. Ed. 53 (2014) 2969-2972.
[93] Q. Zhang, P. Yin, J. Zhang, et al., Cyanoborohydride-based ionic liquids as green aerospace bipropellant fuels, Chemistry 20 (2014) 6909-6914.
[94] S. Chen, Z. Yang, B. Wang, et al., Molecular perovskite high-energetic materials, Sci. China Mater. 61 (2018) 1123-1128.
[95] Y. Shang, R. Huang, S. Chen, et al., Metal-Free Molecular Perovskite High-Energetic Materials, Cryst. Growth Des. 20 (2020) 1891-1897.
[96] S. Chen, Y. Shang, J. Jiang, et al., A new nitrate-based energetic molecular perovskite as a modern edition of black powder, Energetic Mater. Front. 3 (2022) 122-127.
[97] S. Chen, Y. Shang, C. He, et al., Optimizing the oxygen balance by changing the A-site cations in molecular perovskite high-energetic materials, CrystEngComm 20 (2018) 7458-7463.
[98] Y. Shang, S. L. Chen, Z. H. Yu, et al., Silver(I)-Based Molecular Perovskite Energetic Compounds with Exceptional Thermal Stability and Energetic Performance, Inorg. Chem. 61 (2022) 4143-4149.
[99] Z. Yu, D. Liu, Y. Ling, et al., Periodate-based molecular perovskites as promising energetic biocidal agents, Sci. China Mater. 66 (2022) 1641-1648.
[100] T. Wang, Z. Lu, Z. Yi, et al., Study on Primary Explosive: Cu(ClO4)2-Based Energetic Coordination Compounds as a Template, Cryst. Growth Des. 23 (2023) 5528-5534.
[101] S. Li, T. Wang, C. Zhang, et al., Balancing the Energy and Sensitivity of Primary Explosives: Using Isomers to Prepare Energetic Coordination Compounds, Inorg. Chem. 64 (2025) 2020-2029.
[102] C. Zhang, T. Wang, M. Xu, et al., Regulating the Coordination Environment by Using Isomeric Ligands: Enhancing the Energy and Sensitivity of Energetic Coordination Compounds, Inorg. Chem. 62 (2023) 17417-17424.
[103] Z. Lu, T. Wang, M. Sun, et al., Synthesis of energetic coordination compounds based on pyrazole and 4-chloropyrazole via co-melting crystallization method, CrystEngComm 26 (2024) 1178-1188.
[104] M. Friedrich, J. C. Gálvez-Ruiz, T. M. Klapötke, et al., BTA copper complexes, Inorg. Chem. 44 (2005) 8044-8052.
[105] G. H. Tao, D. A. Parrish, J. M. Shreeve, Nitrogen-rich 5-(1-methylhydrazinyl)tetrazole and its copper and silver complexes, Inorg. Chem. 51 (2012) 5305-5312.
[106] S. Cudzilo, M. Nita, Synthesis and explosive properties of copper(II) chlorate(VII) coordination polymer with 4-amino-1,2,4-triazole bridging ligand, J. Hazard. Mater. 177 (2010) 146-149.
[107] B. Wu, T. Zhang, Y. Li, et al., Energetic Compounds Based on 4-Amino-1, 2, 4-triazole (ATZ) and Picrate (PA): [Zn(H2O)6](PA)2·3H2O and [Zn(ATZ)3](PA)2·2.5H2O]n, Z. Anorg. Allg. Chem. 639 (2013) 2209-2215.
[108] O. S. Bushuyev, P. Brown, A. Maiti, et al., Ionic polymers as a new

structural motif for high-energy-density materials, J. Am. Chem. Soc. 134 (2012) 1422-1425.

[109] B. Wu, Y. Bi, F. Li, et al., A Novel Stable High-Nitrogen Energetic Compound: Copper(II) 1,2–Diaminopropane Azide, Z. Anorg. Allg. Chem. 640 (2013) 224-228.

[110] B. Wu, Z. Zhou, F. Li, et al., Preparation, crystal structures, thermal decompositions and explosive properties of two new high-nitrogen azide ethylenediamine energetic compounds, New J. Chem. 37 (2013) 646-653.

[111] C. Xu, J. Zhang, X. Yin, et al., Cd(II) complexes with different nuclearity and dimensionality based on 3-hydrazino-4-amino-1,2,4-triazole, J. Solid State Chem. 226 (2015) 59-65.

[112] X. Liu, W. Gao, P. Sun, et al., Environmentally friendly high-energy MOFs: crystal structures, thermostability, insensitivity and remarkable detonation performances, Green Chem. 17 (2015) 831-836.

[113] Z. Liu, T. Zhang, J. Zhang, et al., Studies on three-dimensional coordination polymer [Cd2(N2H4)2(N3)4]n: crystal structure, thermal decomposition mechanism and explosive properties, J. Hazard. Mater. 154 (2008) 832-838.

[114] S. Wang, F. Zheng, M. Wu, et al., Hydrothermal syntheses, crystal structures and physical properties of a new family of energetic coordination polymers with nitrogen-rich ligand N-[2-(1H-tetrazol-5-yl)ethyl]glycine, CrystEngComm 15 (2013).

[115] S. Li, Y. Wang, C. Qi, et al., 3D energetic metal-organic frameworks: synthesis and properties of high energy materials, Angew. Chem. Int. Ed. 52 (2013) 14031-14035.

[116] S. Zhang, X. Liu, Q. Yang, et al., A new strategy for storage and transportation of sensitive high-energy materials: guest-dependent energy and sensitivity of 3D metal-organic-framework-based energetic compounds, Chemistry 20 (2014) 7906-7910.

[117] J. Song, T. Guo, M. Yao, et al., A comparative study of thermal kinetics and combustion performance of Al/CuO, Al/Fe2O3 and Al/MnO2 nanothermites, Vacuum 176 (2020) 109339.

[118] T. Zhang, Z. Wang, G. Li, et al., Tuning the reactivity of Al/Fe2O3 nanoenergetic materials via an approach combining soft template self-assembly with sol–gel process process, J. Solid State Chem. 230 (2015) 1-7.

[119] X. Ke, X. Zhou, H. Gao, et al., Surface functionalized core/shell structured CuO/Al nanothermite with long-term storage stability and steady combustion performance, Mater. Des. 140 (2018) 179-187.

[120] M. Zaky, A. Elbeih, T. Elshenawy, Review of Nano-thermites; a Pathway to Enhanced Energetic Materials, Cent. Eur. J. Energ. Mater. 18 (2021) 63-85.

[121] M. Wang, W. Xiong, D. Chang, et al., Effect of Microstructure on Energy Release Characteristics of Al/Ni Energetic Structural Material Prepared by Cold Spraying, Langmuir 40 (2024) 18619-18630.

[122] A. Prakash, A. V. McCormick, M. R. Zachariah, Synthesis and Reactivity of a Super-Reactive Metastable Intermolecular Composite Formulation of Al/KMnO4, Adv. Mater. 17 (2005) 900-903.

[123] M. G. Zaky, M. S. Elwesemy, M. Abdelhafiz, et al., The impact of various metals on the performance of TNT, J. Phys. Conf. Ser. 2830 (2024) 012028.

[124] Y. He, X. Wang, Y. Ren, et al., Initial response and combustion behavior of microscale Al/PTFE energetic material by nanosecond laser ignition, Combus. Flame 254 (2023) 112838.

[125] C. Wu, J. Nie, S. Li, et al., μAl-based reactive materials with improved energy efficiency by using the fluorine-containing oxidizer perfluoropolyether as an interfacial layer, Combus. Flame 248 (2023) 112554.

[126] Z. Wu, J. Liu, S. Zhang, et al., Enhanced thermal- and impact-initiated reactions of PTFE/Al energetic materials through ultrasonic-assisted core-shell construction, Def. Technol. 18 (2022) 1362-1368.

[127] K. Gao, G. Li, Y. Luo, et al., Preparation and characterization of the AP/Al/Fe2O3 ternary nano-thermites, J. Therm. Anal. Calorim. 118 (2014) 43-49.

[128] H. Gao, W. Pan, X. Feng, Effect of AP distribution on energy release characteristics and functional force of HMX/AP/Al explosives, Propellants Explos. Pyrotech. 49 (2024) e202300263.

[129] Y. Chen, H. Ren, X. Wu, et al., "Litchi-like" metastable Al/Ti/CuO micro-nano composites with enhanced combustion reaction and their energy characteristics, Combus. Flame 256 (2023) 112947.

[130] Z. Zhuang, K. Xu, B. Liu, et al., Improved reactivity and energy release performance of core-shell structured fuel-rich Si/PTFE energetic composites, Combus. Flame 255 (2023) 112889.

[131] J. C. Quagliano Amado, P. G. Ross, L. Mattos Silva Murakami, et al., Properties of Hydroxyl-Terminal Polybutadiene (HTPB) and Its Use as a Liner and Binder for Composite Propellants: A Review of Recent Advances, Propellants Explos. Pyrotech. 47 (2022) e202100283.

[132] T. Jarosz, A. Stolarczyk, A. Wawrzkiewicz-Jalowiecka, et al., Glycidyl Azide Polymer and its Derivatives-Versatile Binders for Explosives and Pyrotechnics: Tutorial Review of Recent Progress, Molecules 24 (2019) 4475-4520.

[133] P. Kishore, A. Singh, R. Kumar, et al., Effect of curative in hydroxyl-terminated polybutadiene-based binder system on characteristic properties and kinetics of polymer-based energetic composite, J. Energ. Mater. (2024) 1-28.

[134] S. Wang, Y. Zhang, C. Wu, et al., Equal-Material Manufacturing of a Thermoplastic Melt-Cast Explosive Using Thermal-Pressure Coupling Solidification Treatment Technology, ACS Omega 8 (2023) 16251-16262.

[135] J. Zhang, K. He, D. Zhang, et al., Three-dimensional printing of energetic materials: A review, Energetic Mater. Front. 3 (2022) 97-108.

[136] N. Chen, C. He, S. Pang, Additive manufacturing of energetic materials: Tailoring energetic performance via printing, J. Mater. Sci. Technol. 127 (2022) 29-47.